

Multi-Level Power-Imbalance Allocation Control for Secondary Frequency Control in Power Systems

Kaihua Xi, Hai Xiang Lin, Chen Shen, Jan H. van Schuppen,

Abstract—This paper focuses on secondary frequency control of large-scale power systems. First a centralized and a consensus control based distributed control law are presented, then a multi-level control law, named *Multi-Level Power-Imbalance Allocation Control* (MLPIAC), for the large-scale power systems partitioned into more than one region. The centralized and distributed control law are applied within each region and over the regions respectively. Besides restoring nominal frequency with a minimized control cost, MLPIAC also considers the transient behavior of the system after a disturbance. We present a control strategy different from the one applied in the *Power-Imbalance Allocation Control* (PIAC), which also enhances the transient behavior of the frequency through an accelerated convergence of the control inputs eliminating overshoots in MLPIAC. In the level of the distributed control over the regions, the consensus of the marginal costs can be accelerated through a single parameter. Furthermore, because the number of regions is smaller than that of nodes, MLPIAC is more effective to obtain the minimized cost than the purely distributed control law. The asymptotic stability of MLPIAC is proven using the Lyapunov method and the performance is evaluated through simulations.

Index Terms—Power Systems, Secondary Frequency Control, Economic Power Dispatch, Distributed Power-Imbalance Allocation Control, Multi-Level Power-Imbalance Allocation Control

I. INTRODUCTION

Power systems are often geographically extended and supply power to tens of millions of inhabitants and many companies over a large domain. A major objective of the power companies is to provide alternating current at the standard frequency, 60 Hz in the USA, and 50 HZ in the main parts of Europe and in Asia. The power demand fluctuates continuously due to switching on or off machines or computers. Consequently, the frequency of the power systems also fluctuates continuously. So the power grids must be controlled to maintain the frequency as close as possible to the agreed reference value.

For frequency control there are three forms of control: primary, secondary, and tertiary frequency control with control operations distinguished from fast to slow timescales. Primary frequency control is implemented as direct feedback at any power generator to keep the local frequency of the power generator synchronizing near the reference value. Secondary frequency control is implemented also at the local power sources but it takes care of the control task of keeping

the frequency constant in a power system region. Tertiary frequency control addresses the economic performance of the power generators. Each power generator of each power plant has an optimal economic performance at reference values that minimizes the energy losses due to transportation and the economic costs of production while keeping the power supply equal to the power demand.

In this paper the focus is on secondary frequency control. Consider a power system for a large area, partition the area into several (say three to ten) power system regions, and there exist controllers for each of the power system regions and there is a communication network linking all controllers and all busses. The aim is to synthesize a multi-level control law to control the power system so as to achieve the control objective of secondary frequency control. The control objectives can be described as: keep the frequency of the power system as close as possible to the reference value, prevent oscillations and overshoots in the dynamics of frequency, and minimize the economic cost in the operation of the power system. The control law is to be implemented in the form of controllers for each of the power system regions together with a controller for the complete power system area.

The initial approach to control synthesis of a large-scale system is to apply centralized control. Thus, there is one controller which receives information about the frequencies of all buses, hence from all power plants and from all power users as aggregated at buses. The controller is expected to issue control commands to all power plants so that the closed-loop power system meets the control objectives.

For the secondary frequency control of power systems, various centralized control approaches are proposed, including the traditional *Automatic Generation Control* (AGC) [14], *Gather-and-Broadcast Control* (GB) [8] and *Power-Imbalance Allocation Control* [40]. From the global perspective of the entire power system, the AGC method and GB method are a form of integral control. The common drawback of integral control is that large control gain coefficients introduce overshoots and small ones lead to slow convergence. To address the large frequency deviation problem, which is the main concern of power systems integrated with large amounts of renewable, the convergence speed is critical. The *Power-Imbalance Allocation Control* (PIAC) method eliminates the common drawback of the integral control based approaches and improves the transient performance of the power system effectively [40].

In practice today's power systems are becoming so large that they cannot be effectively controlled by a centralized controller. The communication overhead and the control computations to be carried out at the central controller take so

Kaihua Xi, Hai Xiang Lin and Jan H. van Schuppen are with Delft Institute of Applied Mathematics, Delft University of Technology, 2628CD, Delft, The Netherlands (e-mail: K.Xi@tudelft.nl).

Chen Shen is with the State Key Laboratory of Power Systems, Department of Electrical Engineering, Tsinghua University, Beijing, 10084, China.

much time that the control objectives cannot be satisfactorily achieved.

Therefore, a form of decentralized control or distributed control is implemented for control of power systems [22]. The forms of primary and secondary frequency control are motivated by this preference for distributed control. In distributed control there are several controllers in a power system each of which aims to achieve the control objectives for a particular power system region. In addition, the controllers of the various power system regions cooperate with each other to achieve the control objectives for the entire power system area. This paper aims to develop a distributed control approach for a large-scale power system.

Various distributed control approaches for secondary frequency control are proposed in literatures. The *Distributed Averaging Proportional Integral* (DAPI) control is widely studied for traditional power system and Micro-Grids [26], [34], [30], [9], [42]. Based on the principle of consensus control, the objective that the control cost is minimized is achieved by the DAPI method. Considering the congestion problems of the transmission lines, a distributed real-time optimal power flow is proposed in [20]. The approach optimizes the control cost at the steady state avoiding the congestion problem.

Other control approaches are based on primal-dual algorithm [6], e.g., *Economic Automatic Generation Control* (EAGC) approach [18], and a distributed control approach avoiding a congestion problem in [36]. All these approaches can control the power system to a steady state in which the control cost is minimized and the frequency is restored to the nominal frequency. However, the performance of the power systems in the transient phase after a disturbance is not considered at all. Similar to the AGC and GB method, these methods suffer from the common drawback of the integral control that large gain coefficients introduce overshoots. The overshoots lead to the undesired extra oscillations of the frequency of the power system. The potentially promising approach is the *Unified Control* (UC) framework for the primary and secondary frequency control proposed in [43]. It shows through numerical results that the overshoot can be potentially suppressed by the UC framework. However, theoretical analysis on how to improve the transient behavior is absent. The traditional method to eliminate the overshoots is to calculate the gain coefficient by analyzing the eigenvalues of the linearized system as in [37], [38]. However, the eigenvalues are determined by the structure of the control approaches, the improvement of the transient performance obtained by the eigenvalue analysis is not as good as expected. A distributed control approach eliminating the overshoot problem such as the PIAC is required.

Distributed control and decentralized control are subareas of control theory for which a satisfactory and complete control theory does not exist. These problems are difficult because the interactions of the various subsystems are not fully understood and because there is interaction between the controllers via the power system. These topics are the focus of current ongoing research but there is no satisfactory understanding yet. The research area of networked control systems is the focus of intensive research and distributed control of power systems

may benefit from this investigation.

Since the centralized control approach is able to decrease the control cost effectively and the distributed control is powerful for large-scale power systems, we aim to design a multi-level control approach that combines the centralized and distributed control approaches. Both the transient behavior and the steady state of the power system after a disturbance will be considered.

In the paper, first a centralized and a distributed secondary frequency control approach, called *Gather-Broadcast Power-Imbalance Allocation Control* (GBPIAC) and *Distributed Power-Imbalance Allocation Control* (DPIAC) are presented respectively. Both approaches have the nice transient behavior such as in PIAC through an accelerated convergence of the control inputs without any overshoots. Then a multi-level control, *Multi-Level Power-Imbalance Allocation Control* (MLPIAC), which comprises the GBPIAC and DPIAC method for large-scale power systems is proposed. For the MLPIAC method we partition the large-scale power system into a number of regions. There are two control levels in MLPIAC, i.e., control within each region and control over the regions. GBPIAC is implemented within each region and DPIAC over the regions. Within each region, the local control inputs are calculated by solving an economic power dispatch problem. Over the regions, the marginal costs of regions are exchanged via a communication network based on the consensus control principle, thus a consensus marginal cost is achieved at the steady state. So the control cost of the system is minimized at the steady state. As in PIAC, the overshoot of the control inputs are eliminated and the transient behavior of the system can be improved through an accelerated convergence of the control inputs in MLPIAC. Since the scale of the network in the distributed control on the control level over the regions becomes smaller, the marginal cost usually achieves the consensus faster. Furthermore, the consensus speed of the marginal cost can also be accelerated by increasing a single control gain coefficient, which results in a smaller control cost.

To simplify the description of MLPIAC, the two special cases of MLPIAC, the GBPIAC and DPIAC method are introduced before the MLPIAC method. This paper is organized as follows. We describe the dynamic model of the power network in section II, formulate the problem in section III, and propose the GBPIAC and DPIAC method in section IV. We synthesize the MLPIAC method with stability analysis in section V and provide the case study to evaluate the performance of MLPIAC in section VI. Concluding remarks are given in section VII.

II. DYNAMIC MODEL AND THE SYNCHRONIZED STATE OF POWER NETWORKS

A power network is described by a graph $G = (\mathcal{V}, \mathcal{E})$ with nodes \mathcal{V} and edges $\mathcal{E} \subseteq \mathcal{V} \times \mathcal{V}$ where a node represents a bus and edge (i, j) represents the direct transmission line connection between node i and j . The buses may connect to synchronous machines, frequency dependent power sources (e.g., power inverters of renewable energy) or loads, or passive loads. The resistance of the transmission lines are neglected and the susceptance is denoted by \hat{B}_{ij} . Denote the set of

the buses of the synchronous machines, frequency dependent power sources, passive loads by $\mathcal{V}_M, \mathcal{V}_F, \mathcal{V}_P$ respectively, thus $\mathcal{V} = \mathcal{V}_M \cup \mathcal{V}_F \cup \mathcal{V}_P$.

The dynamic model of the power system is described by the following *Differential Algebraic Equations* (DAEs), e.g.,[8],

$$\dot{\theta}_i = \omega_i, \quad i \in \mathcal{V}_M \cup \mathcal{V}_F, \quad (1a)$$

$$M_i \dot{\omega}_i = P_i - D_i \omega_i - \sum_{j \in \mathcal{V}} B_{ij} \sin(\theta_i - \theta_j) + u_i, \quad i \in \mathcal{V}_M, \quad (1b)$$

$$0 = P_i - D_i \omega_i - \sum_{j \in \mathcal{V}} B_{ij} \sin(\theta_i - \theta_j) + u_i, \quad i \in \mathcal{V}_F, \quad (1c)$$

$$0 = P_i - \sum_{j \in \mathcal{V}} B_{ij} \sin(\theta_i - \theta_j), \quad i \in \mathcal{V}_P, \quad (1d)$$

where θ_i is the phase angle at node i , ω_i is the frequency deviation from the nominal frequency, i.e., $f^* = 50$ or 60 Hz, $M_i > 0$ is the moment of inertia of the synchronous machine, D_i is the droop control coefficient, P_i is the power generation (or demand), $B_{ij} = \hat{B}_{ij} V_i V_j$ is the effective susceptance matrix, V_i is the voltage, u_i is the secondary control input. We assume that the nodes participating in the secondary frequency control are equipped with the primary controller. Denote the set of the nodes equipped with the secondary controllers by \mathcal{V}_K , thus $\mathcal{V}_K = \mathcal{V}_M \cup \mathcal{V}_F$. Since the control of the voltage and the frequency can be decoupled, we do not model the dynamics of the voltages and assume the voltage of each bus is a constant which can be derived from power flow calculation [17]. This model and the ones with linearized sine function are widely studied, e.g.,[8], [9], [34], [24], [27], [43], [18], in which the frequency dependent nodes are usually used to model the renewable power inverters.

Similar to the Kuramoto-model [7], the system (1) synchronizes at an equilibrium state, called the *synchronous state* defined as follows.

Definition 2.1: Define a steady state of the power system (1) with constant power loads (generation) such that,

$$\omega_i = \omega_{syn}, \quad i \in \mathcal{V}_M \cup \mathcal{V}_F \quad (2a)$$

$$\dot{\omega}_i = 0, \quad i \in \mathcal{V}_M \cup \mathcal{V}_F, \quad (2b)$$

$$\theta_i = \omega_{syn} t + \theta_i^*, \quad i \in \mathcal{V}, \quad (2c)$$

$$\dot{\theta}_i = \omega_{syn}, \quad (2d)$$

in which θ_i^* is the phase angle of node i at the steady state, $\omega_{syn} \in \mathbb{R}$ is the synchronized frequency deviation.

Note that the angle differences $\{\theta_{ij}^* = \theta_i^* - \theta_j^*, i, j \in \mathcal{E}\}$ determine the power flows in the transmission lines. Substituting (2) into the system (1), we derive the explicit formula of the synchronized frequency deviation as

$$\omega_{syn} = \frac{\sum_{i \in \mathcal{V}} P_i + \sum_{i \in \mathcal{V}_K} u_i}{\sum_{i \in \mathcal{V}_M \cup \mathcal{V}_F} D_i}, \quad (3)$$

which states the necessity of the secondary frequency control. Without the secondary frequency control, i.e., $u_i = 0$ for all $i \in \mathcal{V}_K$, the synchronized frequency deviation $\omega_{syn} \neq 0$ if $\sum_{i \in \mathcal{V}} P_i \neq 0$. The *power imbalance* is defined as $P_s = \sum_{i \in \mathcal{V}} P_i$. In order to avoid damages to the electrical devices in the system, the frequency deviation should be zero, i.e.,

$\omega_{syn} = 0$, for which the necessary condition is

$$P_s + \sum_{i \in \mathcal{V}_K} u_i = 0,$$

which can be satisfied by the value of $\{u_i, i \in \mathcal{V}_K\}$ determined by a control law. When a large amount of renewable energy are integrated into the power system, the power imbalance P_s may fluctuate seriously due to the uncertainty of the weather, which leads to frequency oscillations. We aim to synthesis an effective frequency control law to control ω_{syn} to zero in this paper.

III. SECONDARY FREQUENCY CONTROL

In this section, we introduce the secondary frequency control with the consideration of the economic power dispatch problem and formulate the problems that need to be solved in this paper.

A. Economic power dispatch

In secondary frequency control, a control objective is to minimize the control cost [14] for the following economic power dispatch problem,

$$\begin{aligned} \min_{\{u_i \in \mathbb{R}, i \in \mathcal{V}_K\}} & \sum_{i \in \mathcal{V}_K} J_i(u_i), \\ \text{s.t.} & P_s + \sum_{i \in \mathcal{V}_K} u_i = 0, \end{aligned} \quad (4)$$

where the control costs $J_i(u_i)$ of the controllers are different for various reasons such as different device maintenance prices.

For the secondary frequency control which demands a minimized control cost, we need to solve the following problem.

Problem 3.1: Design a control law for the inputs $\{u_i, i \in \mathcal{V}_K\}$ of the system (1) such that, after a disturbance,

- (i) the state converges to a synchronous state as in (2) with $\omega_{syn} = 0$,
- (ii) the control cost is minimized at the synchronous state, equivalently, the economic power dispatch problem (4) is solved.

Remark 3.2: In tertiary control [20], [43], the congestion problem in the transmission lines and constraints of the control input are considered, in which case the constraints

$$|\theta_{ij}^*| \leq \gamma_{ij} \leq \frac{\pi}{2}, \quad (i, j) \in \mathcal{E}, \quad (5)$$

$$u_i \in [\underline{u}_i, \bar{u}_i], \quad i \in \mathcal{V}_K, \quad (6)$$

are integrated into the optimization problem (4).

Since this paper aims to improve the transient performance, we assume the constraints (5,6) are always satisfied, which can be guaranteed by tertiary control. To simplify the problem, we make the following assumptions for the economic power dispatch problem (4).

Assumption 3.3: For the problem 3.1, we assume

- (i) the power imbalance P_s is a constant,
- (ii) the power imbalance can be compensated by the control inputs such that

$$-P_s \in \left[\sum_{i \in \mathcal{V}_K} \underline{u}_i, \sum_{i \in \mathcal{V}_K} \bar{u}_i \right],$$

(iii) the angle difference $|\theta_{ij}|$ is smaller than γ_{ij} , so the constraints (5) are always satisfied and neglected in this paper.

Problem (4) with Assumption (3.3) is still practical and valuable to be solved as an initial step to realize real-time optimal power flow control for future smart grids, e.g., [9], [14], [24], [34], and Assumption (3.3) is realistic with tertiary control which calculates the operating points for primary control and secondary control.

For solving the optimization problem (4), a necessary condition is [14]

$$J'_i(u_i) = J'_j(u_j) = \lambda, \forall i, j \in \mathcal{V}_K, \quad (7)$$

where $J'_i(u_i) = \frac{dJ_i(u_i)}{du_i}$ is the *marginal cost* of node i for all $i \in \mathcal{V}_K$ and λ is the *nodal price*. In this paper, we consider the quadratic cost functions, $J_i(u_i) = \frac{1}{2}\alpha_i u_i^2$ where α_i is the control price of the controller at node i . Note that if the power imbalance P_s is known, the optimization problem (4) can be solved analytically with the necessary condition (7). However, P_s is unknown in practice since the loads cannot be predicted precisely in a short timescale.

After a disturbance has occurred, the state of the power system experiences two phases: a transient phase and a steady phase. The secondary frequency control solving optimization problem (4) usually considers the steady state only, e.g., [8], [24], [28], [1], [18], [34].

Frequency control treated by optimal control [19], [11] as introduced in Appendix D, concerns primarily the transient phase. In that optimal control framework, the control objective is to minimize the control cost and frequency deviation over a short horizon the constraints are the dynamic equations (1), the inequalities (5), and (6). However, the solution of the optimal secondary frequency control cannot be solved directly since an exact forecast of the fluctuating loads is needed, which is impossible in practice. Alternatively, the performance of the optimal control of the power system can be reached by hierarchical control, i.e., primary, secondary and tertiary control, if the transient performance is properly addressed.

In this paper, besides Problem 3.1 for the steady state, the following problem concerning the transient phase is also considered [41].

Problem 3.4: Design a secondary frequency control law for $\{u_i, i \in \mathcal{V}_K\}$ of system (1) so as to improve the transient performance of the frequency after a disturbance through an accelerated convergence of the control inputs, where the extra oscillation of the frequency caused by the overshoots of the control inputs is eliminated.

To the best of our knowledge, control approaches of the literature do not consider the transient phase and the first solution of Problem 3.4 is the *Power-Imbalance Allocation Control* (PIAC) [40]. For the properties of PIAC, we refer to [41] which also provides the implementation of PIAC in multi-area control and asymptotic stability analysis.

PIAC is a centralized control approach. There is a centralized controller that collects the value of the system state and calculates the local control inputs which are allocated to the local controllers via a communication network. However,

for a large-scale power system, the system is so large that it cannot be effectively controlled by a centralized controller as in PIAC due to the overhead communications and the control computations. Therefore, a form of decentralized control or of distributed control is required for large-scale power systems. Since there is no coordination in decentralized control, the control cost of the power system cannot be minimized by the decentralized control. Hence, we consider distributed control which can minimize the control cost through coordination between the controllers. Notice that the centralized control method can control the system effectively while minimizing the control cost for a large-scale power system. We aim to synthesize a multi-level control law for which the centralized control and distributed control can be implemented flexibly.

B. Multilevel control

Multi-Level control systems have been defined before for several classes of systems [15], [16]. In the past the term *hierarchical system* was used to describe a system with at the highest-level one subsystem, at the next lower level two or more subsystems and the second lower level even more subsystems. The relations of a subsystem with its parent at the next-higher level and its children at the next-lower level have then to be defined. Because we focus on the hierarchy over the network of the power system rather than the one for frequency control with primary, secondary and tertiary control as in [12], [14], the term *multi-level system* will be used in this paper.

Definition 3.5: Define a *multi-level control system architecture* as consisting of a multi-level control system with two, three, or more levels. Below the term control subsystems is abbreviated to subsystem. The highest level is referred to as level 1, the next-highest level as level 2, etc. At the highest level there will be only one subsystem called the main subsystem. At level 2 there may be two or more subsystems. Each subsystem is connected to a parent subsystem at the next higher level and to two or more children subsystems at the next-lower level.

The association with the power system is such that at the lowest level there will be at any subsystem a bus with a power source or a power load, at the next-higher level a subsystem for the regional power subsystem and at the highest level the main subsystem for the area power system. Since centralized control performs well on decreasing the control cost and distributed control is powerful for large-scale systems, so we seek to combine the advantages of both into the multi level control. With a distributed control based on the consensus control principle as in [1], [28], the multi-level control law considers the following problem.

Problem 3.6: Design a secondary frequency control law for $\{u_i, i \in \mathcal{V}_K\}$ of a multi-level power system such that

- (i) the control law over the regions minimizes the control cost of all the regions at the steady state;
- (ii) the control law within each region minimizes the control cost of the local controllers at the steady state;
- (iii) the control law over the regions and the one within each of the regions minimizes the control cost of all the local controllers at the steady state;

- (iv) the transient performance of the controller is improved with an accelerated consensus process.

The focus of this paper is to synthesize a multi-level control law to solve Problem 3.1, 3.4 and 3.6. We first propose a centralized control law, *Gather-Broadcast Power-imbalance Allocation Control* (GBPIAC), and a distributed control law, *Distributed Power-imbalance Allocation Control* (DPIAC), that solves Problem 3.1 and 3.4 as the PIAC method, followed by a multi level control, called *Multi-Level Power-imbalance Allocation Control* (MLPIAC), through combining the two control laws to further solve Problem 3.6. The next subsection introduces the principle of PIAC for solving Problem 3.1 and 3.4, which will be used for the synthesis of the centralized and distributed control approach.

A communication network is required for the control law to solve the economic power dispatch problem (4), for which we make the following assumption.

Assumption 3.7: Consider the system (1) with secondary controllers,

- (i) for the PIAC and GBPIAC method, assume all buses in $\mathcal{V}_M \cup \mathcal{V}_F$ are connected by a communication network and the state information $\{\omega_i, i \in \mathcal{V}_M \cup \mathcal{V}_F\}$ can be collected by a coordinator at a central node and the control inputs $\{u_i, i \in \mathcal{V}_K\}$ can be broadcast by the coordinator to the local controller at node i for all $i \in \mathcal{V}_K$ via the communication network
- (ii) for the DPIAC method, assume all buses in $\mathcal{V}_M \cup \mathcal{V}_F$ are connected by a communication network and node i can exchange the marginal cost λ_i of the node with its neighbors connected through the communication network.
- (iii) for the MLPIAC method, assume that within each power network region all buses with synchronous machines and with frequency dependent devices are connected by a communication network such that the local frequency deviations can be collected by the coordinator and the control commands can be broadcast by the coordinator to the local controllers via the communication network, and assume that over all the regions, the coordinators are connected by a communication network such that the coordinator of a region can exchange the marginal cost of the region to its neighbor regions via the communication network.

With Assumption (3.7), the power system can be viewed as a machine, in which all the state information can be collected and all the disturbances can be estimated accurately via the state information. Furthermore, any region controller can communicate its control commands to all other region controllers and to the area controller. There usually are time-delay and noise in the measurement of the frequency and communications which are neglected in this paper.

C. The PIAC method

In order to explain the idea for eliminating the overshoot of control input, we introduce the PIAC method in this subsection. Inspired by the cruise control of a car [4], the PIAC method is defined as follows [40].

Definition 3.8 (PIAC): For the power system (1) with Assumption (3.3) and (3.7), the PIAC control law is defined as follows.

$$\dot{\eta}(t) = \sum_{i \in \mathcal{V}_M \cup \mathcal{V}_F} D_i \omega_i(t), \quad (8a)$$

$$u_s(t) = -k \left(\eta(t) + \sum_{j \in \mathcal{V}_M} M_j \omega_j(t) \right), \quad (8b)$$

$$u_i(t) = \frac{\alpha_s}{\alpha_i} u_s(t), \quad (8c)$$

$$\frac{1}{\alpha_s} = \sum_{i \in \mathcal{V}_K} \frac{1}{\alpha_i}, \quad (8d)$$

where k is a positive parameter, and the cost functions are quadratic, i.e., $J_i(u_i) = \frac{1}{2} \alpha_i u_i^2$ for $i \in \mathcal{V}_K$.

The total control input $u_s(t)$ is computed by (8b) and then dispatched to every local node $i \in \mathcal{V}$ according to (8c). The properties of PIAC are formulated in the following theorem.

Theorem 3.9: Consider the PIAC control law for the power system (1), the controller has the following properties,

- (a) at any time, $t \in T$, $u_s(t)$ satisfies

$$\dot{u}_s(t) = -k \left(u_s(t) + P_s \right). \quad (9)$$

So $u_s(t)$ converges to $-P_s$ exponentially with a speed determined by k .

- (b) at any time, $t \in T$, the inputs $\{u_i(t), i \in \mathcal{V}_K\}$ solve the following optimization problem,

$$\begin{aligned} \min_{\{u_i \in \mathbb{R}, i \in \mathcal{V}_K\}} \sum_{i \in \mathcal{V}_K} J_i(u_i) \\ \text{s.t.} \quad -u_s(t) + \sum_{i \in \mathcal{V}_K} u_i(t) = 0. \end{aligned} \quad (10)$$

- (c) if there exists a steady state for the system (1) with PIAC, Problem 3.1 is solved, i.e., $\{\omega_i^* = 0, i \in \mathcal{V}_M \cup \mathcal{V}_F\}$, and the optimization problem (4) is solved;
- (d) PIAC is of Proportional-Integral type because

$$u_s(t) = -k \sum_{i \in \mathcal{V}_M} M_i \omega_i - k \int_0^t \sum_{j \in \mathcal{V}_M \cup \mathcal{V}_F} D_j \omega_j dt,$$

For the details of the proof of Theorem (3.9), we refer to [40].

In PIAC, the proportional term $k \sum_{i \in \mathcal{V}_M} M_i \omega_i$ is used to suppress the overshoot of the total control input, and PIAC solves Problem 3.1 and 3.4. However, PIAC is a centralized scheme in which the main control procedure is implemented by a coordinator. A distributed secondary frequency control method is required that inherits the main characteristic of PIAC and avoids the drawback of the traditional secondary frequency control method.

IV. GATHER-BROADCAST AND DISTRIBUTED PIAC

In this section, we introduce the *Gather-broadcast Power-Imbalance Allocation Control* (GBPIAC) and *Distributed Power-Imbalance Allocation Control* (DPIAC) method respectively as a preparation for the multi-level control approach. Both approaches solve Problem 3.1 and 3.4. To simplify the exposition, we first define an abstract frequency deviation for the system in IV-A, then introduce the GBPIAC method,

which inherits the main characteristics of PIAC in IV-B, and introduce the DPIAC method in IV-C.

A. Definition of an abstract frequency deviation

We view the power network as a mechanical bar and define an *abstract frequency deviation* ω_s as follows [41].

Definition 4.1: For the power system (1), an abstract frequency deviation ω_s is defined as follows,

$$M_s \dot{\omega}_s = P_s - D_s \omega_s + u_s \quad (12)$$

where $M_s = \sum_{i \in \mathcal{V}_M} M_i$, $D_s = \sum_{i \in \mathcal{V}} D_i$, and $u_s = \sum_{i \in \mathcal{V}_K} u_i$ is the total control input of the system.

$\omega_s(t)$ is a virtual global frequency deviation, which is different from both $\omega_i(t)$ and $\omega_{syn}(t)$ in general. However, if the power loads (or generation) $\{P_i, i \in \mathcal{V}\}$ change slowly such that the synchronization ω_i is not influenced so much, the differences between $\omega_i(t)$ and $\omega_s(t)$ can be neglected, i.e., $\omega_i(t) = \omega_s(t)$. In that case, summing all the equations in (1), we obtain (12).

It can be easily derived that $\omega_s^* = (P_s + u_s)/D_s$ at the steady state of (12), which leads to $\omega_s^* = \omega_{syn}$ by (3). So controlling ω_s of (12) to zero, i.e., $\lim_{t \rightarrow \infty} \omega_s(t) = 0$, is equivalent to restoring the nominal frequency of the system (1).

As explained in [41], the overshoot of u_s usually causes extra oscillations of the frequency mentioned in Problem 3.4. In order to let u_s converge to $-P_s$ without an overshoot, we construct the following dynamic control law for system (12),

$$\dot{\eta}_s = D_s \omega_s, \quad (13a)$$

$$\dot{\xi}_s = -k_1(M_s \omega_s + \eta_s) - k_2 \xi_s, \quad (13b)$$

$$u_s = k_2 \xi_s. \quad (13c)$$

In the following, we show that the control law (13) eliminates the overshoot problem of u_s of (12) with $k_2 \geq 4k_1$. With the control law (13), the closed-loop system of the system (12) is as follows,

$$M_s \dot{\omega}_s = P_s - D_s \omega_s + k_2 \xi_s, \quad (14a)$$

$$\dot{\eta}_s = D_s \omega_s, \quad (14b)$$

$$\dot{\xi}_s = -k_1(M_s \omega_s + \eta_s) - k_2 \xi_s. \quad (14c)$$

Let $v_s = (M_s \omega_s + \eta_s)$, from (14), it yields

$$\dot{v}_s = P_s + k_2 \xi_s, \quad (15a)$$

$$\dot{\xi}_s = -k_1 v_s - k_2 \xi_s, \quad (15b)$$

from which we derive the dynamics of the control input u_s ,

$$\dot{v}_s = P_s + u_s, \quad (16a)$$

$$\dot{u}_s = -k_2(k_1 v_s - u_s), \quad (16b)$$

where P_s is a constant value. The eigenvalues of the linear system (16) are

$$\mu = \frac{-k_2 \pm \sqrt{k_2^2 - 4k_1 k_2}}{2}. \quad (17)$$

To avoid the extra oscillation caused the overshoot, the imaginary part of the eigenvalues in (17) should be zero, which leads to $k_2 \geq 4k_1$. Hence if $k_2 \geq 4k_1$, u_s converges to $-P_s$

exponentially without any overshoots and subsequently the abstract frequency deviation $\omega_s(t)$ converges to zero without any extra oscillations, thus $\omega_{syn} = 0$. If u_s is known, the control inputs during the transient phase can be computed by solving the optimization problem (10) which is solved by (8c,8d). It follows from (8c,8d) that as $u_s(t)$ converges to $-P_s$ exponentially, $u_i(t)$ also converges to the desired value exponentially with a speed determined by k_1 , thus the extra oscillation of the frequency is avoided. However, u_s cannot be directly calculated as in (12) since ω_s is a virtual frequency deviation and cannot be measured in practice. For the power system (1), the dynamics of the total control input u_s as in (16) is desired to avoid the overshoot in this paper. This is different from the PIAC method with dynamics of u_s as in (9), which will be explained in Remark (4.5) in subsection IV-C. In the following two subsections, we will introduce the GBPIAC and DPIAC method where the total control input u_s also satisfies (16).

B. The centralized control approach: GBPIAC

With the idea of the control law (13) for system (12), we return to the power system (1) and synthesize a control law in which u_s converges to the power imbalance $-P_s$ exponentially as in (16). The GBPIAC method is defined as a dynamic control law as follows.

Definition 4.2 (GBPIAC): Consider the power system (1) of a single region with Assumption (3.3) and (3.7), the GBPIAC control law is defined as the dynamic controller,

$$\dot{\eta}_s = \sum_{i \in \mathcal{V}_F} D_i \omega_i, \quad (18a)$$

$$\dot{\xi}_s = -k_1 \left(\sum_{i \in \mathcal{V}_M} M_i \omega_i + \eta_s \right) - k_2 \xi_s, \quad (18b)$$

$$u_i = \frac{\alpha_s}{\alpha_i} k_2 \xi_s, \quad i \in \mathcal{V}_K, \quad (18c)$$

$$\frac{1}{\alpha_s} = \sum_{i \in \mathcal{V}_K} \frac{1}{\alpha_i}, \quad (18d)$$

where η_s , ξ_s are state variables of the controller, k_1 , k_2 are positive parameters and α_s is a constant.

It can be easily obtained for GBPIAC that $k_2 \xi_s$ provides the total control input at any time $t \in T$, i.e., $k_2 \xi_s(t) = u_s(t)$. The procedure of the centralized control approach (18) is similar to that of the PIAC method. A coordinator first collects the frequency deviations $\{\omega_i, i \in \mathcal{V}_M \cup \mathcal{V}_F\}$, then calculates the total control input $k_2 \xi_s$ by (18a,18b) and local inputs $\{u_i, i \in \mathcal{V}_K\}$ by (18c,18d), finally allocates the control input u_i to the local controller at node i via the communication network.

It will be shown in the next section that GBPIAC is a special case of MLPIAC, in which the power system is controlled as a single area. The properties of GBPIAC follows Theorem 5.2 directly. As illustrated in Theorem 5.2, $\{u_i, i \in \mathcal{V}_K\}$ calculated from (18c) solve the optimization problem (10) at any time $t \in T$, so the marginal costs of all the controller are identical during the transient phase. Furthermore, the total control input u_s satisfies (16), the control gain coefficients should be such that $k_2 \geq 4k_1$ to eliminate the overshoot problem. Because the objective of Problem 3.4 is to avoid the extra oscillation of the

frequency caused by the overshoot of u_s , we set $k_2 = 4k_1$ in the remaining of this paper,

Similar to the PIAC method, the dynamics of the power system can also be decomposed into three sub-processes,

- (i) the convergence process of $u_s(t)$ to $-P_s$ as in (16) with a speed determined by k_1 (or k_2 since $k_2 = 4k_1$).
- (ii) the convergence process of the global frequency deviation $\omega_s(t)$ to zero as in (12) with a speed determined by $u_s(t)$ and D_s .
- (iii) the synchronization process of the local frequency deviation $\omega_i(t)$ to $\omega_s(t)$ which is described by (1), and the speed is determined by $\{u_i(t), i \in \mathcal{V}_K\}$ and $\{D_i, i \in \mathcal{V}_M \cup \mathcal{V}_F\}$. Here, $u_i(t)$ is the solution of the optimization problem (10).

The transient behavior can be improved with GBPIAC by tuning the control parameters $k_1, \{D_i, i \in \mathcal{V}_M \cup \mathcal{V}_F\}$ for the three subprocesses. Similar to PIAC, GBPIAC also focuses on the convergence of u_s and ω_s which can be accelerated with a large k_1 . The synchronization of $\{\omega_i, i \in \mathcal{V}_M \cup \mathcal{V}_F\}$ to ω_s is mainly influenced by $\{D_i, i \in \mathcal{V}_M \cup \mathcal{V}_F\}$ which can be tuned in primary control as in [9], [23].

Theorem 5.2 indicates that the performance of GBPIAC is quite similar to that of PIAC, in which the overshoot problem is avoided and the convergence can be accelerated. This can be observed in the simulations in section VI. Hence Problem 3.4 is solved by GBPIAC. We remark that the influence of k_1 in GBPIAC is similar to k in PIAC on the transient behavior of ω_s , which is analyzed in Appendix B-1.

C. The distributed control approach: DPIAC

In this subsection, we introduce the DPIAC method where the total control input u_s also has the dynamics (16).

Definition 4.3 (DPIAC): Consider the power system (1) where each node is controlled as a region with Assumption (3.3) and (3.7). Define the DPIAC method as a dynamic controller of the form: for each node $i \in \mathcal{V}_K$,

$$\dot{\eta}_i = D_i \omega_i + k_3 \sum_{j \in \mathcal{V}} l_{ij} (k_2 \alpha_i \xi_i - k_2 \alpha_j \xi_j), \quad (19a)$$

$$\dot{\xi}_i = -k_1 (M_i \omega_i + \eta_i) - k_2 \xi_i, \quad (19b)$$

$$u_i = k_2 \xi_i, \quad (19c)$$

where η_i, ξ_i are state variables of the controller, k_1, k_2 and k_3 are positive gain coefficients, (l_{ij}) defines a weighted undirected communication network with Laplacian matrix (L_{ij})

$$L_{ij} = \begin{cases} -l_{ij}, & i \neq j, \\ \sum_{k \neq i} l_{ik}, & i = j, \end{cases} \quad (20)$$

and $l_{ij} \in [0, \infty)$ is the weight of the communication line connecting node i and node j , which is in practice determined by engineers.

In DPIAC, the local controller at node i needs to calculate the control input u_i with locally measured data of ω_i , marginal costs $\alpha_i \xi_i$ and the marginal costs $k_2 \alpha_j \xi_j$ of its neighbours connected by communication lines. Hence no coordinator as in the PIAC and GBPIAC method is needed. However, with the coordination on the marginal costs by the local controllers,

the control cost is minimized at the steady state as the marginal costs achieve a consensus.

It will be shown in the next section that DPIAC is actually a special case of the MLPIAC method, in which each node is controlled as a region. So the properties of DPIAC follows Theorem 5.2 directly. In particular, the dynamics of u_s and ω_s satisfy (16) and (12) respectively, where k_1 determines the convergence speed of $u_s(t)$, and k_1 and D_s determine the convergence speed of $\omega_s(t)$. In this case, DPIAC also eliminates the overshoot of the control input as in GBPIAC.

Unlike GBPIAC, DPIAC involves in the consensus process of the marginal cost $k_2 \alpha_i \xi_i$ with a consensus speed determined by the coefficient k_3 and matrix (L_{ij}) . The decomposition of the dynamics of the power system controlled by DPIAC is summarized as follows.

- (i) the convergence process of $u_s(t)$ to $-P_s$ as in (16) with a convergence speed determined by k_1 .
- (ii) the convergence process of the global frequency deviation $\omega_s(t)$ to zero as in (12) with a convergence speed determined by $u_s(t)$ and D_s .
- (iii) the synchronization process of the local frequency deviation $\omega_i(t)$ to $\omega_s(t)$ which is described by (32), and the synchronization speed is determined by $u_i(t)$ and $\{D_i, i \in \mathcal{V}_M \cup \mathcal{V}_F\}$.
- (iv) the consensus process of the marginal cost $k_2 \alpha_i u_i(t)$ with a consensus speed determined by k_3 and (L_{ij}) .

We remark that with the same values of k_1 and D_s , the control cost of DPIAC is larger than that of GBPIAC since the optimization problem (10) is not solved simultaneously in the transient phase as in GBPIAC. However, with a larger coefficient k_3 , the marginal costs reach consensus faster and the control cost of DPIAC becomes smaller. This is analyzed in Appendix B-2 for the system where the frequencies synchronize much faster than the consensus speed of the marginal cost. Hence, to obtain a fast consensus speed of the marginal cost, the gain coefficient k_3 should be increased.

Remark 4.4: Without the coordination on the marginal costs of nodes, DPIAC reduces to a decentralized control method as follows

$$\dot{\eta}_i = D_i \omega_i, \quad (21a)$$

$$\dot{\xi}_i = -k_1 (M_i \omega_i + \eta_i) - k_2 \xi_i, \quad (21b)$$

$$u_i = k_2 \xi_i \quad (21c)$$

in which the abstract standard frequency deviation ω_s behaves identically as that of DPIAC and of GBPIAC even though the economic dispatch problem is not solved.

In the optimal control framework (91) of Appendix D, the control objective actually is a trade-off between the cost of the control and all the local frequency deviations, which is determined by R_1 and R_2 in (91). In DPIAC, the trade-off can be determined by the control coefficient k_1, k_3 , which will be explained in the case study in section VI.

The following remark explains the motivation of the introduction of ξ_s in (13) and the dynamics of u_s in (13).

Remark 4.5: To utilize the consensus principle, the state variable ξ_i is introduced in DPIAC. This is practical since ξ_i can be used to describe the dynamics of the generator turbine

which is neglected in (1)[17], [35]. In this case, it is natural to introduce ξ_s in (18) in order to evaluate the global performance of DPIAC on the abstract standard frequency deviation ω_s . On the other hand, without introducing ξ_i , as in the DAPI method [27], the variable η_i for the integral control can be exchanged between the nodes in the distributed control with the form

$$\dot{\eta}_i = D_i \omega_i + k_3 \sum_{j \in \mathcal{V}} l_{ij} (\alpha_i \eta_i - \alpha_j \eta_j) \quad (22a)$$

$$u_i = -k M_i \omega_i - k \eta_i. \quad (22b)$$

where the term $-k M_i \omega_i$ is added to the secondary control input $u_i(t)$ such that u_s converges to $-P_s$ exponentially without an overshoot as in (9). Hence the behavior of the abstract frequency deviation ω_s is similar as in GBPIAC and DPIAC. However, $-\sum_{i \in \mathcal{V}_K} k \eta_i$ does not estimate the power imbalance P_s in the transient phase, thus the control cost cannot be decreased by increasing the gain coefficient k_3 .

V. MULTILEVEL CONTROL APPROACH

In this section, we introduce the *Multi-Level Power Imbalance Allocation Control* (MLPIAC) for secondary frequency control of the power system.

For a large-scale power system A , we partition the network into m regions such that

$$A = A_1 \cup \dots \cup A_r \cup \dots \cup A_m, \quad Z_m = \{1, 2, \dots, m\}, \quad (23a)$$

$$A_r \cap A_q = \emptyset, \quad \forall r \neq q, \quad r, q \in Z_m. \quad (23b)$$

Denote the set of the nodes in region A_r by \mathcal{V}_{A_r} , the nodes of the synchronous machine by \mathcal{V}_{M_r} , the nodes of the frequency dependent power sources by \mathcal{V}_{F_r} and the nodes with secondary controller by \mathcal{V}_{K_r} . Denote the marginal cost of region A_r by λ_r . Z_{m_r} as the set of the neighbor regions of region A_r connected by communication lines.

We refer the control over the regions to as level 1 and the control within the region as level 2 and the primary control at a node in a region as level 3. The diagram in Fig. 1 illustrates the control architecture of MLPIAC. MLPIAC focuses on the secondary frequency at level 1 and 2. In MLPIAC, the centralized control method GBPIAC is implemented within each region at level 2 and the distributed control method DPIAC is implemented between the regions at level 1.

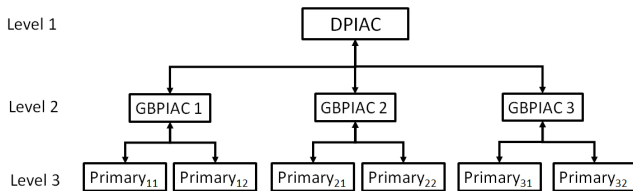


Fig. 1. Diagram of the multi-level control of power systems.

The MLPIAC method is defined as follows.

Definition 5.1 (MLPIAC): Consider a large-scale power system (1) with Assumption (3.3) and (3.7), which is partitioned

as in (23). At level 2, the dynamic control law in region A_r is described by the equations

$$\dot{\eta}_r = \sum_{i \in \mathcal{V}_{M_r} \cup \mathcal{V}_{F_r}} D_i \omega_i + k_3 v_r, \quad (24a)$$

$$\dot{\xi}_r = -k_1 \left(\sum_{i \in \mathcal{V}_{M_r}} M_i \omega_i + \eta_r \right) - k_2 \xi_r, \quad (24b)$$

$$0 = \frac{\lambda_r}{\alpha_r} - k_2 \xi_r, \quad (24c)$$

$$u_i = \frac{\lambda_r}{\alpha_i}, \quad i \in \mathcal{V}_{K_r}, \quad (24d)$$

$$\frac{1}{\alpha_r} = \sum_{i \in \mathcal{V}_{K_r}} \frac{1}{\alpha_i} \quad (24e)$$

where η_r, ξ_r are state variables of the controller, v_r is an algebraic variable, $k_1, k_2, k_3 \in (0, \infty)$ are parameters, α_r is a constant defined as the control price of region A_r . At level 1, the coordinator of the regions is an algebraic equation only

$$v_r = \sum_{A_q \subset A} l_{rq} (\lambda_r(t) - \lambda_q(t)) \quad (25a)$$

with as input of the coordinator, $\{\lambda_r(t), \forall r \in Z_m\}$ and as output of the coordinator $\{v_r(t), \forall r \in Z_m\}$. l_{rq} defines a weighted undirected communication network with Laplacian matrix $(L_{rq}) \in \mathbb{R}^{m \times m}$

$$L_{rq} = \begin{cases} -l_{rq}, & r \neq q, \\ \sum_{k \neq i} l_{rk}, & r = q, \end{cases} \quad (26)$$

and $l_{rq} \in [0, \infty)$ is the weight of the communication line connecting region A_r and node A_q .

In MLPIAC, at level 2, within a region A_r , a coordinator collects the local frequency deviation $\{\omega_i, i \in \mathcal{V}_M \cup \mathcal{V}_F\}$ and calculates the region control input $k_2 \xi_r = \sum_{i \in \mathcal{V}_{K_r}} u_i$ by (24a, 24b), the marginal cost of the region λ_r by (24c) and the local control input $\{u_i, i \in \mathcal{V}_{K_r}\}$ by (24d). In the remaining of the paper, we denote the total control input of region A_r by $u_r = k_2 \xi_r$.

In MLPIAC, at level 1, the coordinators of the regions exchange the marginal cost in order to achieve a consensus marginal cost which is a necessary condition for the global economic power dispatch as stated in (7).

Before analyzing the properties of MLPIAC at the transient phase and steady state, we focus on the partition of the network. For the large-scale power system, the multi-level control approach (24) reduces to the DPIAC method (19) if each region consists of a single node, where as it reduces to the GBPIAC method (18) if the entire network is controlled as a single region. Hence the DPIAC and GBPIAC methods are two special cases of MLPIAC.

Theorem 5.2: Consider a large-scale power system partitioned as in (23), the controller of the MLPIAC method has the following properties,

- at any time $t \in T$, the total control input u_s of the system satisfies (16), thus it converges to $-P_s$ exponentially if $k_2 \geq 4k_1$;
- at any time $t \in T$, within a region A_r , the inputs $\{u_i, i \in$

\mathcal{V}_{K_r} of the local controllers solve the following economic power dispatch problem

$$\begin{aligned} \min_{\{u_i \in \mathbb{R}, i \in \mathcal{V}_{K_r}\}} \sum_{i \in \mathcal{V}_{K_r}} J_i(u_i) \quad (27) \\ \text{s.t.} \quad -u_r(t) + \sum_{i \in \mathcal{V}_{K_r}} u_i(t) = 0. \end{aligned}$$

(c) if there exists a steady state as in (2) for the system, Problem 3.1 is solved, i.e., $\{\omega_i^* = 0, i \in \mathcal{V}_M \cup \mathcal{V}_F\}$ and the optimization problem (4) is solved.

Proof: (a) By definition of the Laplacian matrix $(L_{rq}) \in \mathbb{R}^{m \times m}$ in (26), we derive that

$$\sum_{r,q \in Z_m} L_{rq}(\lambda_r - \lambda_q) = 0. \quad (28)$$

Summing all the equations in (1), we obtain

$$\sum_{i \in \mathcal{V}_M} M_i \dot{\omega}_i = P_s - \sum_{i \in \mathcal{V}_M \cup \mathcal{V}_F} D_i \omega_i + u_s. \quad (29)$$

Summing all the control inputs $\{u_r, r \in Z_m\}$ with $u_r = k_2 \xi_r$, we derive the total control input of the system as $u_s = \sum_{r \in Z_m} k_2 \xi_r$. It follows from (28) and (24b) that

$$\dot{u}_s(t) = -k_2 \left(k_1 \left(\sum_{i \in \mathcal{V}_M} M_i \omega_i + \eta_s \right) + u_s(t) \right), \quad (30)$$

where $\eta_s = \sum_{r \in Z_m} \eta_r$ and following (24a) with derivative

$$\dot{\eta}_s = \sum_{i \in \mathcal{V}_M \cup \mathcal{V}_F} D_i \omega_i \quad (31)$$

Let $v_s(t) = \sum_{i \in \mathcal{V}_M} M_i \omega_i + \eta_s$, we derive (16a) from (29) and (31), and (16b) from (30). Hence u_s satisfies (16). Following the formula (17) of the eigenvalues, we derive that u_s converges to $-P_s$ exponentially without any overshoots if $k_2 \geq 4k_1$.

(b) Following (24d), we derive that at any time $t \in T$,

$$\alpha_i u_i = \alpha_j u_j = \alpha_r k_2 \xi_r, \forall i, j \in \mathcal{V}_{K_r}.$$

So the necessary condition (7) for the optimization problem (27) is satisfied. Further with $\sum_{i \in \mathcal{V}_{K_r}} u_i(t) = u_r(t)$, we obtain that the optimization problem (27) is solved at any time t .

(c) This follows Proposition 5.4 directly. \square

With MLPIAC (24), the dynamics of the power system can also be decomposed into 4 subprocesses as that of DPIAC (19). However, the consensus process concerns the regions' marginal costs $\{\lambda_r, A_r \subset A\}$ with consensus speed determined by k_3 and (L_{rq}) . In this case, as in DPIAC, the transient behavior of the power system controlled by MLPIAC can also be greatly improved by tuning the related coefficients of the 4 subprocesses, i.e., the primary control focuses on the synchronization of the frequencies, in which the transient behavior can be improved by tuning the parameters $\{D_i, i \in \mathcal{V}_M \cup \mathcal{V}_F\}$ as in [9], [23], the secondary control focuses on recovering the nominal frequency, in which the convergence of the control input can be accelerated by a large k_1 eliminating the extra oscillation of the frequency. Hence, Problem 3.4 is solved by MLPIAC. The analysis of the influences of k_1 and k_3 on the transient behavior of ω_s and the consensus speed of

the marginal cost in Appendix B-1 and B-2. So the consensus speed of the marginal cost can be also accelerated by a large k_3 as in DPIAC. Furthermore, for a system with several regions, the scale of the communication network with Laplacian matrix (l_{rq}) is much smaller than the one in the DPIAC method, the speed of achieving a consensus marginal cost of the regions is much faster in MLPIAC. Hence Problem 3.6 is solved by MLPIAC.

Since the transient performance of the frequency can be improved by tuning corresponding control gain coefficients, the trade-off between the control cost and all the local frequency deviation as in the frame work of the optimal control can be determined by k_1 and k_3 . This will be further discussed in the case study in section VI.

Before introducing Proposition 5.4 which illustrates the properties of the steady state of the power system controlled by MLPIAC, we introduce the closed-loop system as follows.

$$\dot{\theta}_i = \omega_i, i \in \mathcal{V}_M \cup \mathcal{V}_F, \quad (32a)$$

$$M_i \dot{\omega}_i = P_i - D_i \omega_i - \sum_{j \in \mathcal{V}} B_{ij} \sin \theta_{ij} + \frac{\alpha_r}{\alpha_i} k_2 \xi_r, i \in \mathcal{V}_{M_r} \subset \mathcal{V}_M, \quad (32b)$$

$$0 = P_i - D_i \omega_i - \sum_{j \in \mathcal{V}} B_{ij} \sin \theta_{ij} + \frac{\alpha_r}{\alpha_i} k_2 \xi_r, i \in \mathcal{V}_{F_r} \subset \mathcal{V}_F, \quad (32c)$$

$$0 = P_i - \sum_{j \in \mathcal{V}} B_{ij} \sin \theta_{ij}, i \in \mathcal{V}_P, \quad (32d)$$

$$\dot{\eta}_r = \sum_{i \in \mathcal{V}_{M_r} \cup \mathcal{V}_{F_r}} D_i \omega_i + k_2 k_3 \sum_{q \in Z_m} l_{rq} (\alpha_r \xi_r - \alpha_q \xi_q), r \in Z_m, \quad (32e)$$

$$\dot{\xi}_r = -k_1 \left(\sum_{i \in \mathcal{V}_{M_r}} M_i \omega_i + \eta_r \right) - k_2 \xi_r, r \in Z_m \quad (32f)$$

where $\theta_{ij} = \theta_i - \theta_j$ for $(i, j) \in \mathcal{E}$.

We focus on the synchronous state of the closed-loop system (32). As in the Kuramoto-model [7], the closed-loop system (32) may not have a synchronous state if the power injections $\{P_i, i \in \mathcal{V}\}$ are much larger than the line capacity $\{B_{ij}, (i, j) \in \mathcal{E}\}$. For more details of the synchronous state of the power systems and Kuramoto-model, we refer to [9] and [39]. So we make an assumption for the power system to ensure there exists a synchronous state, which can be satisfied by reserving some margin of the line capacity in tertiary control which calculates the operating point of the primary and secondary frequency control.

Assumption 5.3: there exists a synchronous state for the closed-loop system (32) such that

$$\theta^* \in \Theta = \left\{ \theta_i \in \mathbb{R}, \forall i \in \mathcal{V} \mid |\theta_i - \theta_j| < \frac{\pi}{2}, \forall (i, j) \in \mathcal{E} \right\}$$

where $\theta^* = \text{col}(\theta_i^*) \in \mathbb{R}^{n_t}$, n_t is the total number of nodes in \mathcal{V} . The condition $\theta^* \in \Theta$ is commonly referred to as a security constraint [24] and restricts the space of the equilibrium to desired power flows.

Note that the equilibria with θ out of Θ usually leads to undesired power flows which either have cyclic power flows or be unstable [39].

For the synchronous state of the closed-loop system, we have the following proposition.

Proposition 5.4: If the assumptions (3.3), (3.7) and (5.3) hold, then there exists at most one synchronous state for the closed-loop system (32) such that

$$\theta_i^* \in \Theta, i \in \mathcal{V} \quad (33a)$$

$$\omega_i^* = 0, \mathcal{V}_M \cup \mathcal{V}_F, \quad (33b)$$

$$P_s + k_2 \sum_{r \in \mathcal{Z}_m} \xi_r^* = 0, \quad (33c)$$

$$k_1 \eta_r^* + k_2 \xi_r^* = 0, r \in \mathcal{Z}_m, \quad (33d)$$

$$\alpha_r \xi_r^* - \alpha_q \xi_q^* = 0, \forall r, q \in \mathcal{Z}_m, \quad (33e)$$

$$\alpha_i u_i^* - k_2 \alpha_r \xi_r^* = 0, i \in \mathcal{V}_{K_r} \subset \mathcal{V}_K. \quad (33f)$$

Proof: It follows Theorem 5.2 that the dynamics of u_s satisfies (16), which yields that $u_s^* = -P_s$ at the synchronous state. Thus (33c) is derived with $u_s(t) = \sum_{r \in \mathcal{Z}_m} k_2 \xi_r(t)$. Following (3), we further derive that $\omega_{syn} = 0$, which yields (33b) with the definition of the synchronous state (2). By (32f), $\omega_i^* = 0$ and $\xi_i^* = 0$ for all $i \in \mathcal{V}_K$, we derive (33d). By (32e) and $\omega_i^* = 0$, we obtain (33e). By (24c) and (24d), we arrive at (33f). From (33e,33f) it follows that $\alpha_i u_i^* = \alpha_j u_j^*$ for all $i, j \in \mathcal{V}_K$, thus the necessary condition (7) is satisfied. Following (33c), it yields $P + \sum_{i \in \mathcal{V}_K} u_i^* = 0$ and the economic dispatch problem (4) is solved subsequently. It follows [3], [31] that there exists at most one synchronous state such that $\theta^* \in \Theta$. \square

In the following, we focus on the asymptotic stability of MLPIAC. The power flows $\{B_{ij} \sin(\theta_{ij}), (i, j) \in \mathcal{E}\}$ only depend on the angle differences. As in [40], we choose a reference angle $\theta_1 \in \mathcal{V}_M$ and transform the system into a new coordinate such that

$$\varphi_i = \theta_i - \theta_1, i \in \mathcal{V}.$$

which yields $\dot{\varphi}_i = \omega_i - \omega_1$ for all i in $\mathcal{V}_M \cup \mathcal{V}_F$. In the new coordinate, the closed-loop system (32) becomes

$$\dot{\varphi}_i = \omega_i - \omega_1, i \in \mathcal{V}_M \cup \mathcal{V}_F, \quad (34a)$$

$$M_i \dot{\omega}_i = P_i - D_i \omega_i - \sum_{j \in \mathcal{V}} B_{ij} \sin \varphi_{ij} + \frac{\alpha_r}{\alpha_i} k_2 \xi_r, i \in \mathcal{V}_M, \quad (34b)$$

$$D_i \dot{\varphi}_i = P_i - D_i \omega_1 - \sum_{j \in \mathcal{V}} B_{ij} \sin \varphi_{ij} + \frac{\alpha_r}{\alpha_i} k_2 \xi_r, i \in \mathcal{V}_F, \quad (34c)$$

$$0 = P_i - \sum_{j \in \mathcal{V}} B_{ij} \sin \varphi_{ij}, i \in \mathcal{V}_P, \quad (34d)$$

$$\dot{\eta}_r = \sum_{i \in \mathcal{V}_{M_r} \cup \mathcal{V}_{F_r}} D_i \omega_i + k_2 k_3 \sum_{q \in \mathcal{Z}_m} l_{rq} (\alpha_r \xi_r - \alpha_q \xi_q), r \in \mathcal{Z}_m, \quad (34e)$$

$$\dot{\xi}_r = -k_1 \left(\sum_{i \in \mathcal{V}_{M_r}} M_i \omega_i + \eta_r \right) - k_2 \xi_r, r \in \mathcal{Z}_m \quad (34f)$$

which is in the form of DAEs (92) of Appendix E, i.e., the algebraic equations are (34d) and algebraic variables are $\varphi_i, i \in \mathcal{V}_P$. Following Assumption (5.3), φ_i satisfies

$$\varphi \in \Phi = \left\{ \varphi_i \in \mathbb{R}, i \in \mathcal{V} \mid |\varphi_i - \varphi_j| \leq \frac{\pi}{2}, \forall (i, j) \in \mathcal{E}, \varphi_1 = 0 \right\}.$$

where $\varphi = \text{col}(\varphi_i) \in \mathbb{R}^{n_r}$.

We make the following assumption on the control gain coefficients k_1, k_2, k_3 as a sufficient condition of the asymptotic stability of MLPIAC in the analysis in Appendix C.

Assumption 5.5: Assume the control gain coefficients,

k_1, k_2, k_3 , satisfy that

$$\frac{k_2}{k_1} > \frac{2(\alpha D)_{\max}}{(\alpha D)_{\min}(1 + 2k_3 \lambda_{\min})}$$

where $(\alpha D)_{\min} = \min\{\alpha_i D_i, i \in \mathcal{V}_K\}$, $(\alpha D)_{\max} = \max\{\alpha_i D_i, i \in \mathcal{V}_K\}$ and λ_{\min} is the smallest nonzero eigenvalue of matrix $L \alpha_R$ where $L = (L_{rq}) \in \mathbb{R}^{m \times m}$ is defined in (26) and $\alpha_R = \text{diag}(\alpha_r) \in \mathbb{R}^{m \times m}$.

We rewrite the state and algebraic variables into a vector form, $(\varphi, \omega, \eta, \xi) \in \mathbb{R}^{n_r} \times \mathbb{R}^n \times \mathbb{R}^m \times \mathbb{R}^m$. The following theorem illustrates the asymptotic stability of the equilibrium of MLPIAC.

Theorem 5.6: If assumptions (3.3,3.7,5.3) and (5.5) hold, then for the closed-loop system (32),

- there exists a unique synchronous state $z^* = (\varphi^*, \omega^*, \eta^*, \xi^*) \in \Psi$ where $\Psi = \Phi \times \mathbb{R}^n \times \mathbb{R}^m \times \mathbb{R}^m$.
- there exists a domain $\Psi^d \subset \Psi$ such that starting at any initial state $z^0 = (\varphi^0, \omega^0, \eta^0, \xi^0) \in \Psi^d$ which satisfies the algebraic equations (34d), the state trajectory converges to the unique synchronous state $z^* \in \Psi$.

The proof of Theorem (5.6) is provided in Appendix C.

Remark 5.7: In MLPIAC, Assumptions (3.3, 3.7, 5.3) and (5.5) are both necessary and realistic at the same time. Assumptions (3.3) and (3.7) are necessary for the implementation of MLPIAC to solve Problem 3.1 where the congestion problem as in (5) is not considered. Assumptions (5.3) and (5.5) are general sufficient conditions for the stability of MLPIAC. Assumption (3.3) and (5.3) can be guaranteed by tertiary control and Assumption (3.7) by an effective communication infrastructure. Regarding Assumption (5.5), we refer to Remark 5.8.

Remark 5.8: The inverse of damping coefficient, $\frac{1}{D_i}$ can be viewed as the control cost of primary control [9]. When $\alpha = \gamma D^{-1}$, $\gamma \in \mathbb{R}$ is a positive number, which indicates the secondary frequency control prices are proportional to the primary control price and leads to $(\alpha D)_{\min} = (\alpha D)_{\max}$, DPIAC is asymptotically stable if $k_2 > 2k_1$. Specially, Assumption (5.5) is relaxed in the GBPIAC method in the theoretical analysis as explained in Remark (C.3) in Appendix C. For DPIAC and MLPIAC, our initial numerical simulations and numerical eigenvalue analysis of the linearized system of (32) have shown that the control law is asymptotically stable even though assumption (5.5) is not satisfied. This will be shown in section VI.

Remark 5.9: The total control input u_s satisfies (9), which is different from (16) in DPIAC, PIAC is not compatible with DPIAC in the multi-level control where the areas cooperate with each other to minimize the control cost of the whole network. However, they are compatible for the power system with multi areas which is controlled in a non-cooperative way as the multi-area control method in [41]. In that case, the controllers in an area only respond to the disturbances occurring in the area.

VI. CASE STUDY

In this section, we evaluate the performance of the multi-level control approach, MLPIAC, on the IEEE-39 buses system

as shown in Fig. 2. The GBPIAC and DPIAC method are two special cases of the MLPIAC method, so we compare the GBPIAC method (18), the DPIAC method (19) and the MLPIAC method (24) by observing the sub-processes identified in section IV respectively. The data of the test system are from [5]. The system consists of 10 generators, 39 buses, which serves a total load of about 6 GW. The voltage at each bus is a constant which is derived by power flow calculation with PSAT [21]. There are 49 nodes in the network including 10 nodes of generators and 39 nodes of buses. In order to involve the frequency dependent power sources, we change the buses which are not connected to synchronous machines into frequency dependent loads. Hence $\mathcal{V}_M = \{G1, G2, G3, G4, G5, G6, G7, G8, G9, G10\}$, $\mathcal{V}_P = \{30, 31, 32, 33, 34, 35, 36, 37, 38, 39\}$ and the other nodes are in set \mathcal{V}_F . The nodes in $\mathcal{V}_M \cup \mathcal{V}_F$ are all equipped with secondary frequency controllers such that $\mathcal{V}_K = \mathcal{V}_M \cup \mathcal{V}_F$. We remark that each synchronous machine is connected to a bus and its phase angle is rigidly tied to the rotor angle of the bus if the voltages of the system are constants, e.g., the classical model of synchronous machine [14]. Thus the angles of the synchronous machine and the bus have the same dynamics. The droop control coefficients are set to be $D_i = 1$ (p.u./p.u. frequency deviation) for all $i \in \mathcal{V}_M \cup \mathcal{V}_F$ under the power base 100 MVA and frequency base 60 Hz. The economic power dispatch coefficient $\alpha_i = 1/\beta_i$ where β_i is generated randomly with a uniform distribution on $(0, 1)$. In the simulations, the setting of $\{D_i, i \in \mathcal{V}_K\}$ and randomly generated coefficient $\{\alpha_i, i \in \mathcal{V}_K\}$ yield that $(\alpha D)_{\min} = 1.0$ and $(\alpha D)_{\max} = 608.9$. The communication network is assumed to be a spanning tree network as shown by the red lines in Fig. 2 and the requirement on the communication network in Assumption (3.7) is satisfied with the spanning tree network. For the GBPIAC method, the entire network is controlled as a single region. For the DPIAC method, each node $i \in \mathcal{V}_K$ is controlled as a single region. For the MLPIAC method, the network is divided into three regions by the dash-dotted black lines as shown in Fig. 2.

We set $l_{ij} = 1$ if node i and j are connected by a communication line in DPIAC (19) and set $l_{r,q} = 1$ if region r and q are connected by a communication line in MLPIAC (24). Note that region 1 and 2 are connected by communication line (1, 2) and region 1 and 3 are connected by (4, 14). However, region 1 and 3 are not connected by a communication line directly. So the marginal cost cannot be exchanged between region 1 and 3. With the control prices α and the Laplacian matrix of the communication network, it can be computed that $\lambda_{\min} = 0.0365$ for DPIAC and $\lambda_{\min} = 0.1933$ for MLPIAC.

At the beginning of the simulations, the power generation and loads are balanced with nominal frequency $f^* = 60$. At time $t = 0.5$ second, the loads at each of the buses 4, 12 and 20 increase 33 MW step-wisely, which amounts to a total power imbalance of 99MW and causes the frequency to drop below the nominal frequency.

In the following, we first evaluate the performance of the control approaches on restoring the nominal frequency with a minimized control cost and then discuss how the control gain coefficients k_1, k_3 influence the transient behaviors of the state of the power system. Note that the topology of the

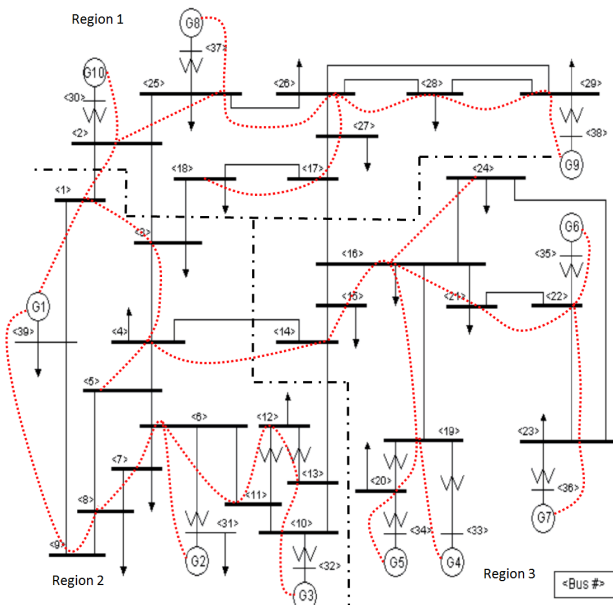


Fig. 2. IEEE New England test power system

communication network and the weight l_{ij} also influence the transient behaviors, which however is not the main concern of this paper. Besides the three sub-processes shared with GBPIAC, i.e., the convergence processes of $u_s(t)$ to $-P_s$, $\omega_s(t)$ to zero, and the synchronization process of ω_i to $\omega_s(t)$, DPIAC considers the consensus process of the marginal costs of all the local nodes and MLPIAC considers the consensus process of the marginal costs of all the regions. On the dynamics of the frequency, we focus on the dynamics of the frequency $\bar{\omega}_i(t) = \omega_i(t) + f^*$ and abstract frequency $\bar{\omega}_s(t) = \omega_s(t) + f^*$ instead of $\omega_i(t)$ and $\omega_s(t)$ respectively. Here, the response of ω_s are obtained from (12) with u_s as the total control input of the three methods respectively. For illustrations of the extra oscillation of frequency caused by the overshoot of u_s , we refer to the simulations in, e.g., [9], [18], [34], [41], [42].

The results are shown in Fig. 3 where there are 20 plots in 5 rows and 4 columns. The plots in the rows from top to bottom illustrate the dynamics of the frequency $\bar{\omega}_i(t) \in \mathcal{V}_M$, control input $u_s(t)$, abstract standard frequency $\bar{\omega}_s(t)$, relative frequency $\omega_i(t) - \omega_s(t)$ for all $i \in \mathcal{V}_M$, and marginal costs of the controllers at the nodes of the synchronous machines in DPIAC and of the regions in MLPIAC, and the plots in the column from left to right illustrate the results of GBPIAC, DPIAC with $k_3 = 5$, DPIAC with $k_3 = 25$, and MLPIAC control with $k_3 = 5$ respectively. In these four simulations, $k_1 = 5, k_2 = 20$. Note that Assumption (5.5) is not satisfied in the simulations of DPIAC and MLPIAC, i.e., $\frac{k_2}{k_1} = 4$ while the values of $\frac{2(\alpha D)_{\max}}{(\alpha D)_{\min} + 2k_3 \lambda_{\min}}$ are about 430 and 414 for DPIAC and MLPIAC respectively. We remark that the relative frequency describes the synchronization process of $\omega_i(t)$ to $\omega_s(t)$, which is the main concern of primary control.

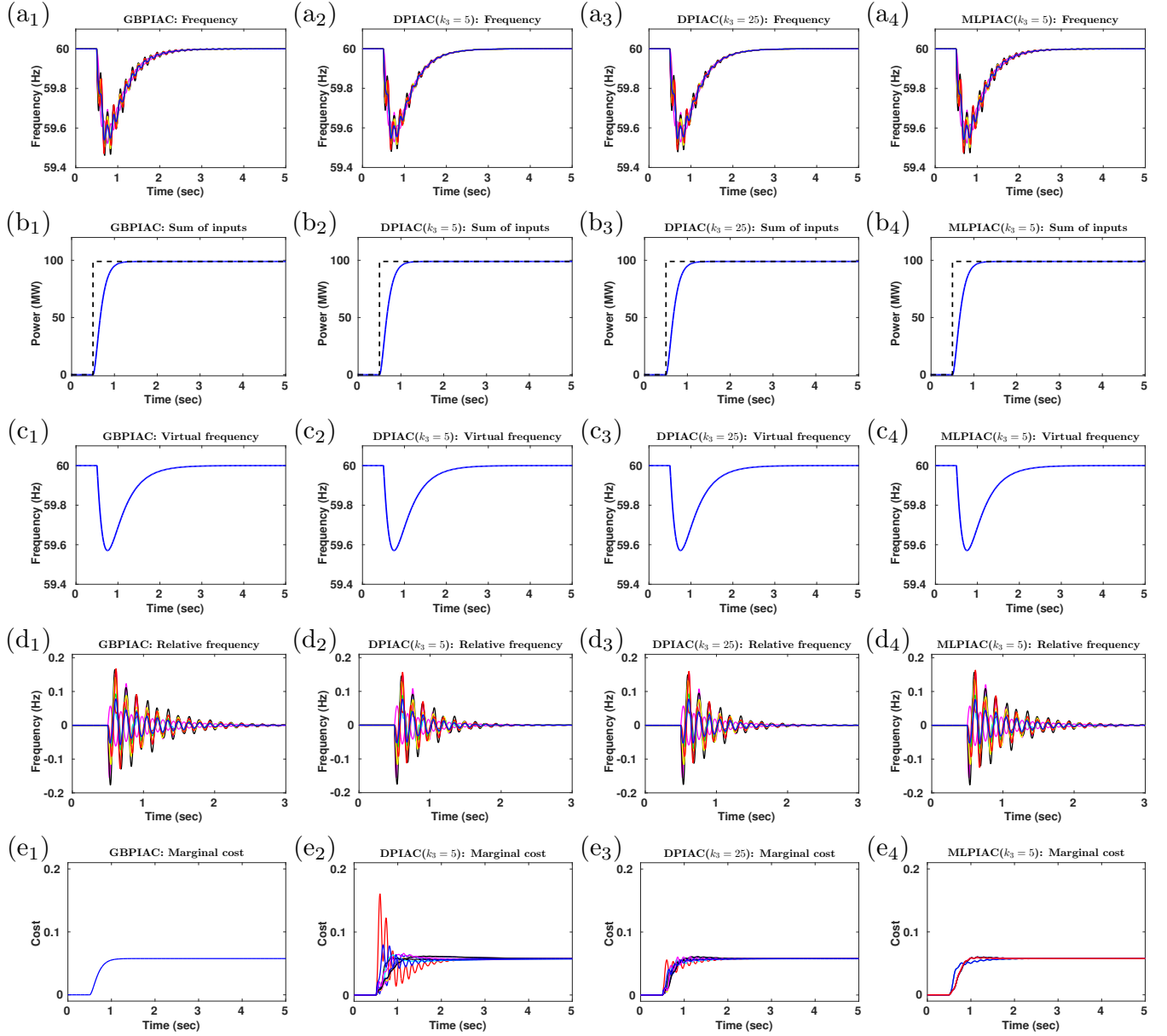


Fig. 3. The simulation results of the GBPIAC, DPIAC and MLPIAC method with $k_1 = 5$, $k_2 = 20$ on IEEE 39-bus test system. The black dashed lines in b_1 - b_4 , denote the power imbalance of the network.

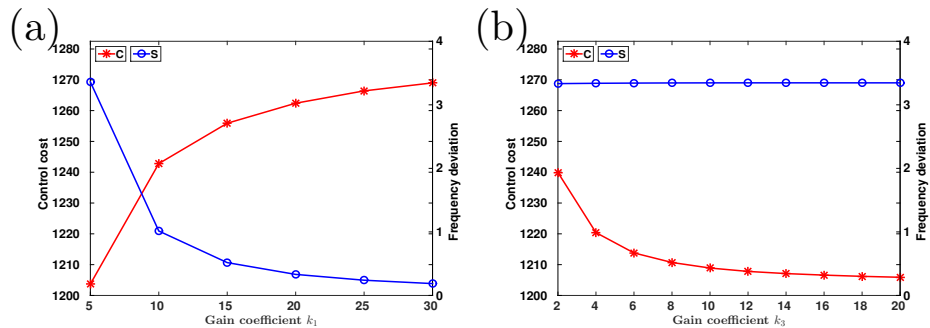


Fig. 4. (a). The cost S of frequency deviations and the cost C of the control input as functions of k_1 (see (35) and (36)). The results are of the GBPIAC method. (b). S and C as functions of k_3 . The results are of the DPIAC method.

Let us first focus on the performance of GBPIAC in the plots in the first column. It can be observed from the plots from top to bottom that the frequencies are restored to the nominal frequency without any extra oscillations, the control input converges to the power imbalance exponentially without an overshoot, the abstract standard frequency converges to the nominal frequency without an overshoot, the frequencies synchronize to the abstract frequency ω_s , the marginal costs are identical at the nodes of the synchronous machines. Hence the performance of GBPIAC is similar to that of PIAC method [40]. So GBPIAC solves Problem 3.1 and 3.4.

Second, we turn to the performance of DPIAC method in the plots in the second and third columns. Compared with the GBPIAC method by observing the plots from top to bottom, the dynamics of $\bar{\omega}_i$ are similar as in GBPIAC, the control input $u_s(t)$ and $\bar{\omega}_s(t)$ are identical to that in GBPIAC, the synchronization of ω_i to ω_s is similar as in GBPIAC with a little bit smaller magnitude of oscillations, the marginal costs are identical at the steady state. However, the marginal costs are not identical in the transient phase, which is different from that in GBPIAC. By comparing result of DPIAC method with $k_3 = 5$ and $k_3 = 25$ in the second and third column, it can be found that the consensus speed of the marginal cost is accelerated and the control cost in the transient phase is decreased by a large k_3 . This verifies the analysis of the influence of k_3 on the transient behavior of the marginal cost in Appendix B-2. However, the coefficient k_3 does not influence the synchronization of ω_i so much by comparing the subprocess of the synchronization of $\omega_i(t)$ to $\omega_s(t)$.

Third, we observe the performance of the MLPIAC method. It can be seen from Fig. 3a₄, Fig. 3b₄, Fig. 3c₄ and Fig. 3d₄ that, the subprocesses of $u_s(t)$, $\omega_s(t)$ and $\omega_i - \omega_s$ are similar as in GBPIAC and DPIAC. However, the marginal costs of the three regions shown in Fig. 3e₄ achieve consensus much faster than in the DPIAC method even though the control gain k_3 for the consensus process equals to the one in DPIAC method. Hence, for a large-scale network, *the multi-level control is more effective in decreasing the control cost than the distributed method.*

Regarding the theoretical analysis in the decomposition of the dynamics of the power system with a communication network, the transient performance depends on the control gain coefficient, k_1 and k_3 . In the following, we explain how the trade-off between the frequency deviation and the control cost can be determined by the control coefficient k_1 and k_3 .

Following the objective of the optimal control in (91) in Appendix D, which is actually the trade-off of the cost between the control input and the state. We calculate the cost of the frequency deviation of the nodes in $\mathcal{V}_M \cup \mathcal{V}_F$ during the transient by

$$S = \sum_{i \in \mathcal{V}_M \cup \mathcal{V}_F} \int_0^{T_0} \omega_i^2(t) dt \quad (35)$$

and the control cost by

$$C = \sum_{i \in \mathcal{V}_M \cup \mathcal{V}_F} \int_0^{T_0} \frac{1}{2} \alpha_i u_i^2(t) dt \quad (36)$$

where the simulation time T_0 is taken to be 5 seconds in our case.

We investigate the influence of k_1 on the trade-off in the GBPIAC method and that of k_3 in the DPIAC. Fig. 4a shows the cost of the control input C and the frequency deviation S as functions of k_1 . It can be observed in Fig. 4a that as k_1 increases, the control cost over the transient phase also increases while the cost of the frequency deviations S decreases. The extreme case where the cost of frequency deviation is required to be arbitrarily small, the k_1 must be arbitrarily large. On the contrast, if the control cost is required to be small, k_1 should be close to zero where the frequency deviation will be very large. Fig. 4b indicates that k_3 does not have as much influence to the cost of frequency deviation S as to the control cost C . As the k_3 increases, the consensus speed increases leading to a small control cost. Hence, the trade-off depends on the control gain coefficients. By tuning the control coefficients k_1 and k_3 in DPIAC, we can obtain a similar transient performance of the power system as in the optimal control where the trade-off is determined by the matrix R_1 and R_2 .

VII. CONCLUSION

In this paper, we proposed a multi-level secondary frequency control, called *Multi-Level Power-Imbalance Allocation control* (MLPIAC), for a large-scale power system consisting of synchronous machines, frequency dependent power sources and passive nodes. For a power system partitioned into several regions, a centralized control approach, GBPIAC, is implemented within each region and a consensus control based distributed control approach, DPIAC, is implemented over the regions. At the steady state, the nominal frequency is restored with a minimized control cost and at the transient phase, the transient behavior of the system can be improved by tuning the control gain coefficients. Because the convergence of the total control input of the system can be accelerated without an overshoot by increasing the gain coefficient k_1 , the extra oscillations of the frequency caused by the overshoot is eliminated, thus as in PIAC [41] the transient behavior of the frequency is improved. Because the consensus of the marginal costs of the regions can be accelerated by increasing the gain coefficient k_3 , the minimized control cost can be obtained faster. Hence, in MLPIAC, the trade-off between the control cost and transient behavior of the frequency can be determined by the control gain coefficients. Furthermore, the large-scale network can be controlled with a minimized cost more effectively than the purely distributed control due to the number of regions is smaller than that of nodes in the system.

However, Assumption (5.5) is still required in the theoretical analysis of asymptotic stability of MLPIAC even though it is not required in the numerical simulations. How to relax Assumption (5.5) theoretically still needs further consideration. Furthermore, there usually are time-delays in the measurement of the frequency and communications in practice, in which case the robustness of MLPIAC needs to be evaluated.

ACKNOWLEDGMENT

The authors thank Dr. Johan L. A. Dubbeldam from Delft University of Technology, Prof. Tongchao Lu from Shandong University, Mr. César A. Uribe from University of Illinois for their useful discussions on this research, including the control algorithm synthesis and stability analysis. Kaihua Xi thanks the China Scholarship Council for the financial support.

REFERENCES

- [1] M. Andreasson, D. V. Dimarogonas, H. Sandberg, and K. H. Johansson. Distributed control of networked dynamical systems: Static feedback, integral action and consensus. *IEEE Transactions on Automatic Control*, 59(7):1750–1764, 2014.
- [2] M. Andreasson, E. Tegling, H. Sandberg, and K. H. Johansson. Coherence in synchronizing power networks with distributed integral control. *arXiv:1703.10425*, 2017.
- [3] A. Araposthatis, S. Sastry, and P. Varaiya. Analysis of power-flow equation. *International Journal of Electrical Power & Energy Systems*, 3(3):115–126, 1981.
- [4] K. J. Aström and R. M. Murray. *Feedback Systems: An introduction for scientists and Engineers*. Princeton, NJ: Princeton UP, 2008.
- [5] T. Athay, R. Podmore, and S. Virmani. A practical method for the direct analysis of transient stability. *IEEE Transactions on Power Apparatus and Systems*, PAS-98(2):573–584, 1979.
- [6] S. Boyd, N. Parikh, E. Chu, B. Peleato, and J. Eckstein. Distributed optimization and statistical learning via the alternating direction method of multipliers. *Foundations and Trends in Machine Learning*, 3(1):1–122, 2010.
- [7] F. Dörfler and F. Bullo. Synchronization in complex networks of phase oscillators: A survey. *Automatica*, 50(6):1539 – 1564, 2014.
- [8] F. Dörfler and S. Grammatico. Gather-and-broadcast frequency control in power systems. *Automatica*, 79:296 – 305, 2017.
- [9] F. Dörfler, J. W. Simpson-Porco, and F. Bullo. Breaking the hierarchy: distributed control and economic optimality in microgrids. *IEEE Transactions on Control of Network Systems*, 3(3):241–253, 2016.
- [10] J. C. Doyle, K. Glover, P. P. Khargonekar, and B. A. Francis. State-space solutions to standard H2 and H infinity control problems. *IEEE Transactions on Automatic Control*, 34(8):831–847, Aug 1989.
- [11] W.H. Fleming and R. W. Rishel. *Deterministic and stochastic optimal control*. Springer-Verlag, 1975.
- [12] J. M. Guerrero, J. C. Vasquez, José Matas, Luis García de Vicuna, and Miguel Castilla. Hierarchical control of droop-controlled ac and dc microgrids—a general approach toward standardization. *IEEE Transactions on Industrial Electronics*, 58(1):158–172, 2011.
- [13] D. J. Hill and I. M. Y. Mareels. Stability theory for differential algebraic systems with applications to power systems. *IEEE Trans. Circuits and Systems*, 37(11):1416–1423, 1990.
- [14] M.D. Ilić and J. Zaborszky. *Dynamics and control of large electric power systems*. John Wiley & Sons, 2000.
- [15] P. L. Kempker, A. C. M. Ran, and J. H. van Schuppen. Lq control for coordinated linear systems. *IEEE Transactions on Automatic Control*, 59(4):851–862, 2014.
- [16] J. Komenda, T. Masopust, and J. H. van Schuppen. Multilevel coordination control of modular des. In *52nd IEEE Conference on Decision and Control*, pages 6323–6328, 2013.
- [17] P. Kundur. *Power system stability and control*. McGraw-Hill, 1994.
- [18] N. Li, C. Zhao, and L. Chen. Connecting automatic generation control and economic dispatch from an optimization view. *IEEE Transactions on Control of Networked Systems*, 3(3):254–263, 2016.
- [19] F. Liu, Y. H. Song, J. Ma, S. Mei, and Q. Lu. Optimal load-frequency control in restructured power systems. *IEE Proceedings - Generation, Transmission and Distribution*, 150(1):87–95, 2003.
- [20] Y. Liu, Z. Qu, H. Xin, and D. Gan. Distributed real-time optimal power flow control in smart grid. *IEEE Transactions on Power Systems*, 32(5):3403–3414, 2017.
- [21] F. Milano. *Power systems analysis toolbox*. University of Castilla, Castilla-La Mancha, Spain, 2008.
- [22] D. K. Molzahn, F. Dörfler, H. Sandberg, S. H. Low, S. Chakrabarti, R. Baldick, and J. Lavaei. A survey of distributed optimization and control algorithms for electric power systems. *IEEE Transactions on Smart Grid*, PP(99):1–1, 2017.
- [23] A. E. Motter, S. A. Myers, M. Anghel, and T. Nishikawa. Spontaneous synchrony in power-grid networks. *Nature Physics*, 9(3):191–197, 2013.
- [24] C. De Persis and N. Monshizadeh. Bregman storage functions for microgrid control. *IEEE Transactions on Automatic Control*, PP(99):1–1, 2017.
- [25] B. K. Poolla, S. Bolognani, and F. Dörfler. Optimal placement of virtual inertia in power grids. *IEEE Transactions on Automatic Control*, PP(99):1–1, 2017.
- [26] J. Schiffer and F. Dörfler. On stability of a distributed averaging PI frequency and active power controlled differential-algebraic power system model. In *European Control Conference*, 2016.
- [27] J. Schiffer, F. Dörfler, and E. Fridman. Robustness of distributed averaging control in power systems: Time delays & dynamic communication topology. *Automatica*, 80:261–271, 2017.
- [28] J. Schiffer, T. Seel, J. Raisch, and T. Sezi. Voltage stability and reactive power sharing in inverter-based microgrids with consensus-based distributed voltage control. *IEEE Transactions on Control Systems Technology*, 24(1):96–109, 2016.
- [29] J. W. Simpson-Porco, B. K. Poolla, N. Monshizadeh, and F. Dörfler. Quadratic performance of primal-dual methods with application to secondary frequency control of power systems. In *2016 IEEE 55th Conference on Decision and Control (CDC)*, pages 1840–1845, Dec 2016.
- [30] J. W. Simpson-Porco, Q. Shafiee, F. Dörfler, J. C. Vasquez, J. M. Guerrero, and F. Bullo. Secondary frequency and voltage control of islanded microgrids via distributed averaging. *IEEE Transactions on Industrial Electronics*, 62(11):7025–7038, 2015.
- [31] S. J. Skar. Stability of multi-machine power systems with nontrivial transfer conductances. *SIAM Journal on Applied Mathematics*, 39(3):475–491, 1980.
- [32] E. Tegling, B. Bamieh, and D. F. Gayme. The price of synchrony: Evaluating the resistive losses in synchronizing power networks. *IEEE Transactions on Control of Network Systems*, 2(3):254–266, Sept 2015.
- [33] Rosario Toscano. *Structured controllers for uncertain systems*. Springer-verlag, London, 2013.
- [34] S. Trip, M. Bürger, and C. De Persis. An internal model approach to (optimal) frequency regulation in power grids with time-varying voltages. *Automatica*, 64:240 – 253, 2016.
- [35] S. Trip and C. De Persis. Optimal frequency regulation in nonlinear structure preserving power networks including turbine dynamics: An incremental passivity approach. In *2016 American Control Conference (ACC)*, pages 4132–4137, 2016.
- [36] Z. Wang, F. Liu, S. H. Low, C. Zhao, and S. Mei. Distributed frequency control with operational constraints, part ii: Network power balance. *IEEE Transactions on Smart Grid*, PP(99):1–1, 2017.
- [37] X. Wu, F. Dörfler, and M. R. Jovanovic. Input-Output analysis and decentralized optimal control of inter-area oscillations in power systems. *IEEE Transactions on Power Systems*, 31(3):2434–2444, 2016.
- [38] X. Wu and C. Shen. Distributed optimal control for stability enhancement of microgrids with multiple distributed generators. *IEEE Transactions on Power Systems*, 32(5):4045–4059, 2017.
- [39] K. Xi, J. L. A. Dubbeldam, and H. X. Lin. Synchronization of cyclic power grids: equilibria and stability of the synchronous state. *Chaos*, 27(1):013109, 2017.
- [40] K. Xi, J. L. A. Dubbeldam, H. X. Lin, and J. H. van Schuppen. Power imbalance allocation control for secondary frequency control of power systems. In *the 20th IFAC World Congress, Toulouse, France*, pages 4466–4471, 2017.
- [41] K. Xi, H. X. Lin, and J. H. van Schuppen. Power imbalance allocation control of power systems—secondary frequency control. *arXiv:1703.02855*, 2017.
- [42] C. Zhao, E. Mallada, and F. Dörfler. Distributed frequency control for stability and economic dispatch in power networks. Chicago, 2015. In *American Control Conference*.
- [43] C. Zhao, E. Mallada, S. Low, and J. Bialek. A unified framework for frequency control and congestion management. In *2016 Power Systems Computation Conference (PSCC)*, pages 1–7, 2016.

APPENDIX A

NOTATIONS FOR THE POWER SYSTEM AND CONTROLLER

To simplify the explanation on the influence analysis of the control gain coefficients and stability analysis of the control law, we introduce the notations for the power system and control laws. The notations are valid for Appendices B, C.

Denote the number of nodes in the sets $\mathcal{V}_M, \mathcal{V}_F, \mathcal{V}_P$ and \mathcal{V}_K by n_m, n_f, n_p, n respectively, the total number of buses in the power system by n_t . So $n = n_m + n_f$ and $n_t = n_m + n_f + n_p$.

To express simply, we write a diagonal matrix $\beta = \text{diag}(\{\beta_i, i \cdots n\}) \in \mathbb{R}^{n \times n}$ with $\beta_i \in \mathbb{R}$ as $\text{diag}(\beta_i)$. It is convenient to introduce the matrices $D = \text{diag}(D_i) \in \mathbb{R}^{n \times n}$, $M = \text{diag}(M_i) \in \mathbb{R}^{n \times n}$, $\alpha = \text{diag}(\alpha_i) \in \mathbb{R}^{n \times n}$. Denote the identity matrix by $I_n \in \mathbb{R}^{n \times n}$. Note that $M_i = 0$ for $i \in \mathcal{V}_F$ and $M_i > 0$ for $i \in \mathcal{V}_M$. Denote the n dimension vector with all elements equal to one by 1_n . Denote $\theta = \text{col}(\theta_i) \in \mathbb{R}^{n_t}$, $\omega = \text{col}(\omega_i) \in \mathbb{R}^n$, $P = \text{col}(P_i) \in \mathbb{R}^{n_t}$ and $\varphi = \text{col}(\varphi_i) \in \mathbb{R}^{n_t}$ where $\varphi_i = \theta_i - \theta_1$ for all $i \in \mathcal{V}$. Denote $\eta = \text{col}(\eta_i) \in \mathbb{R}^n$, $\xi = \text{col}(\xi_i) \in \mathbb{R}^n$.

The number of regions is denoted by m , the control price of region r is α_r . Denote $\alpha_R = \text{diag}(\alpha_r) \in \mathbb{R}^{m \times m}$. Define matrix $R = (r_{ir}) \in \mathbb{R}^{n \times m}$ with $r_{ir} = 1$ if node i belongs to region r , otherwise $r_{ir} = 0$. Note that α, α_R, R satisfy

$$R^T \alpha^{-1} R = \alpha_R^{-1}, \quad (37a)$$

$$1_n = R 1_m. \quad (37b)$$

Denote $L \in \mathbb{R}^{m \times m}$ as the Laplacian matrix of the communication network as defined in (26).

For symmetric matrices A and B , we say $A > 0$ (or $A \geq 0$ if A is positive-definite (or semi-positive-definite)), and say $A > B$ (or $A \geq B$) if $(A - B)$ is positive-definite (or semi-positive-definite).

The following inequality is used frequently in the following stability analysis of the control laws. For any $x \in \mathbb{R}^m, y \in \mathbb{R}^m$, the following inequality holds

$$x^T y \leq \frac{1}{2} x^T \varepsilon x + \frac{1}{2} y^T \varepsilon^{-1} y,$$

where $\varepsilon \in \mathbb{R}^{m \times m}$ is an invertible positive-definite diagonal matrix. The inequality follows from

$$\begin{bmatrix} x \\ y \end{bmatrix}^T \begin{bmatrix} \varepsilon & -I_m \\ -I_m & \varepsilon^{-1} \end{bmatrix} \begin{bmatrix} x \\ y \end{bmatrix} \geq 0.$$

APPENDIX B

SETTING OF THE CONTROL GAIN COEFFICIENTS

In this section, we investigate the influence of the control gain coefficient k_1 and k_3 on the transient behavior of the power system controlled by the MLPIAC method. Subsections B-1 focuses on the transient behavior of the abstract frequency deviation ω_s defined in (12). Subsection B-2 focuses on the transient behavior of the consensus process of the marginal cost in DPIAC and MLPIAC. To simplify the analysis, we make the following assumption for the synchronization of the power system.

Assumption B.1: Assume that the frequency of the power system synchronizes quickly such that the differences between ω_i and ω_s is relatively small compared to ω_s for all $i \in \mathcal{V}_M \cup$

\mathcal{V}_F and can be neglected, or, equivalently $\omega_i = \omega_s$ for $i \in \mathcal{V}_M \cup \mathcal{V}_F$.

Note that the synchronization process of the frequencies is also influenced by the control inputs $\{u_i, i \in \mathcal{V}_K\}$. As u_i changes slowly, the frequencies still can be close to a synchronized state. Hence, Assumption (B.1) is realistic for the case that the frequencies are synchronized while the marginal costs are not synchronized.

B-1 The control gain coefficient k_1

In practice, the frequency of the power system usually synchronizes quickly and the differences between ω_i and ω_s can be neglected as in Assumption (B.1). So it is practical to investigate how k_1 influences the abstract frequency deviation ω_s in GBPIAC, DPIAC and MLPIAC. The dynamics of ω_s under control of GBPIAC, DPIAC and MLPIAC are identical, which can be described by (14). In the following, we investigate the \mathcal{H}^2 norm of ω_s as output of (14) where P_s is the input. The system (14) is rewritten in a general form

$$\dot{x} = Ax + BP_s, \quad (38)$$

$$y = Cx,$$

with

$$x = \begin{bmatrix} \tilde{\omega}_s \\ \eta_s \\ \xi_s \end{bmatrix}, A = \begin{bmatrix} -\frac{D_s}{M_s} & 0 & 4k_1 \\ \frac{D_s}{M_s} & 0 & 0 \\ -k_1 & -k_1 & -4k_1 \end{bmatrix}, B = \begin{bmatrix} 1 \\ 0 \\ 0 \end{bmatrix}, C^T = \begin{bmatrix} \frac{1}{M_s} \\ 0 \\ 0 \end{bmatrix},$$

$\tilde{\omega}_s = M_s \omega_s$, $y = \tilde{\omega}_s / M_s = \omega_s$, $k_2 = 4k_1$. It can be easily verified that A is Hurwitz by calculating the eigenvalues of A .

When P_s is modeled as a Gaussian white noise, setting $y = \omega_s$ and following (98), we derive

$$\lim_{t \rightarrow +\infty} E[|\omega_s(t)|^2] = \text{tr}(B^T Q_t B) = \frac{D_s + 5M_s k_1}{2M_s(2k_1 M_s + D_s)^2}, \quad (39)$$

which indicates that $\omega_s(t)$ can be controlled to any desired range by tuning the coefficient k_1 . Similarly, setting $y(t) = 4k_1 \xi$, we derive the expected value of $\|u_s(t)\|^2 = \|4k_1 \xi_s\|^2$ as

$$\lim_{t \rightarrow +\infty} E[|u_s(t)|^2] = \frac{k_1}{2}, \quad (40)$$

which indicates that as k_1 increases, the expected control input also increases. By (39) and (40), it confirms that the tradeoff between the expected frequency deviation ω_s and the control input u_s can be tuned by k_1 . We remark that the above analysis is valid for the abstract frequency deviation ω_s only. How coefficient k_1 influences the frequency deviation $\omega = \text{col}(\omega_i)$ needs further consideration.

B-2 The control gain coefficient k_3

In this subsection, we investigate the influence of the control gain coefficient k_3 on the consensus speed of the marginal costs in the DPIAC method. The corresponding result can be obtained for the MLPIAC method analogously. Note that $\alpha_R = \alpha$ in DPIAC.

With the notations in Appendix A, the control law (19) is

rewritten in a vector form as follows

$$\dot{\eta} = D\omega + k_2 k_3 L \alpha \xi, \quad (41a)$$

$$\dot{\xi} = -k_1 M \omega - k_1 \eta - k_2 \xi, \quad (41b)$$

$$y = k_2 L \alpha \xi, \quad (41c)$$

where y is the output used to measure the differences of the marginal cost at time t . When P_s is modeled as a Gaussian white noise, $E[|y(t)|^2]$ measures the expected consensus speed of the marginal cost. We evaluate the relationship between $E[|y(t)|^2]$ and k_3 .

Let $\rho = Q^{-1}\eta$ and $\sigma = Q^{-1}\xi$ where Q diagonalizes the symmetrizable matrix $L\alpha$ as in Theorem (F.2). Note that when each node is controlled as a region, we have $\alpha = \alpha_R$ and $R = I_n$ in (37). The system (41) becomes

$$\dot{\rho} = Q^{-1}D\omega + k_2 k_3 \Lambda \sigma, \quad (42a)$$

$$\dot{\sigma} = -k_1 Q^{-1}M\omega - k_1 \rho - k_2 \sigma, \quad (42b)$$

where Λ is a diagonal matrix defined in (94). So the components (ρ_i, σ_i) , $i = 2, \dots, n$, of ρ and σ are decoupled from each other. However, they are still coupled by the frequency deviation ω .

With $Q_{v1} = 1_n$ and $\lambda_1 = 0$, we derive

$$\dot{\rho}_1 = 1_n^T D \omega, \quad (43a)$$

$$\dot{\sigma}_1 = -k_1 1_n^T M \omega - k_1 \rho_1 - k_2 \sigma_1, \quad (43b)$$

for the scalar variable ρ_1 and σ_1 . With assumption (B.1), the dynamics of ω_s is described by (12). Replacing all the frequency deviation $\{\omega_i, i \in \mathcal{V}_M \cup \mathcal{V}_F\}$ by ω_s and following (42) and (43), we derive a closed-loop system controlled by DPIAC as follows,

$$M_s \dot{\omega}_s = P_s - D_s \omega_s - k_2 \sigma_1, \quad (44a)$$

$$\dot{\rho}_1 = D_s \omega_s, \quad (44b)$$

$$\dot{\sigma}_1 = -k_1 M_s \omega_s - k_1 \rho_1 - k_2 \sigma_1, \quad (44c)$$

$$\dot{\rho}_i = c_{1i} \omega_s + k_2 k_3 \lambda_i \sigma_i, \quad i = 2, \dots, n, \quad (44d)$$

$$\dot{\sigma}_i = -k_1 c_{2i} \omega_s - k_1 \rho_i - k_2 \sigma_i, \quad i = 2, \dots, n, \quad (44e)$$

where $c_{1i} = Q_{vi}^T \text{col}(D_i)$ and $c_{2i} = Q_{vi}^T \text{col}(M_i)$.

Let us focus on the output y in (41), we have

$$\begin{aligned} y^T(t)y(t) &= k_2^2 \xi^T \alpha L L \alpha \xi = k_2^2 \sigma^T Q^T \alpha L L \alpha Q \sigma \\ &\quad \text{by (95d).} \\ &= k_2^2 \sigma^T Q^T \alpha L (Q^{-1})^T \alpha^{-1} Q^{-1} L \alpha Q \sigma \\ &= k_2^2 \sigma^T \Lambda^2 \alpha^{-1} \sigma = \sum_{i=2}^n k_2^2 \lambda_i^2 \alpha_i^{-1} \sigma_i^2. \end{aligned}$$

Hence, we only need to calculate $E[|k_2 \lambda_i \sqrt{\alpha_i^{-1}} \sigma_i(t)|^2]$ for all $i = 2, \dots, n$ as an alternative of evaluating $E[|y(t)|^2]$ directly. Setting $k_2 = 4k_1$, we rewrite (44) for component i of vector ρ and σ in the general form (97) with

$$x = \begin{bmatrix} \tilde{\omega}_s \\ \rho_1 \\ \sigma_1 \\ \rho_i \\ \sigma_i \end{bmatrix}, A = \begin{bmatrix} -\frac{D_s}{M_s} & 0 & 4k_1 & 0 & 0 \\ \frac{D_s}{M_s} & 0 & 0 & 0 & 0 \\ -k_1 & -k_1 & -4k_1 & 0 & 0 \\ c_{1i} & 0 & 0 & 0 & 4k_1 k_3 \lambda_i \\ -k_1 c_{2i} & 0 & 0 & -k_1 & -4k_1 \end{bmatrix}, B = \begin{bmatrix} 1 \\ 0 \\ 0 \\ 0 \\ 0 \end{bmatrix},$$

$C = [0, 0, 0, 0, k_2 \lambda_i \sqrt{\alpha_i^{-1}}]$, $\tilde{\omega}_s = M_s \omega_s$, and the stochastic input is P_s . It is obvious that A is Hurwitz by calculating the eigenvalues of it. Following (98), we derive that

$$\lim_{t \rightarrow +\infty} E[|k_2 \lambda_i \sqrt{\alpha_i^{-1}} \sigma_i|^2] = \text{tr}(B^T Q_i B) = \frac{k_1 \lambda_i^2 (b_1 + b_2 + b_3)}{2\alpha_i e_1 e_2 e_3}, \quad (46)$$

where

$$b_1 = c_{1i}^2 \left((D_s/M_s + 4k_1)^2 (k_3 + 9) + 8k_1^2 k_3 \lambda_i \right),$$

$$b_2 = 4c_{2i}^2 k_1^2 (k_3 \lambda_i + 3)^2 (4D/M_s + D_s^2/M_s^2),$$

$$b_3 = 8c_{2i}^2 k_1^2 \left(k_3 \lambda_i (D_s/M_s + 3k_1)^2 + k_1^2 k_3 \lambda_i (2k_3 \lambda_i + 9) \right),$$

$$e_1 = (D_s/M_s + 2k_1)^2,$$

$$e_2 = ((D_s/M_s)^2 + 4D_s k_1/M_s + 4k_3 \lambda_i k_1^2),$$

$$e_3 = (\lambda_i k_3 + 3)^2.$$

It follows from (46) that

$$\lim_{t \rightarrow +\infty} E[|k_2 \lambda_i \sqrt{\alpha_i^{-1}} \sigma_i(t)|^2] = O(k_3^{-1}),$$

which indicates that as k_3 increases, the differences of the marginal costs decrease. Hence k_3 can be tuned to increase the consensus speed of the marginal costs. Similar result can be obtained for MLPIAC directly by setting $c_{1i} = Q_{vi}^T R^T \text{col}(D_i)$ and $c_{2i} = Q_{vi}^T R^T \text{col}(M_i)$ in (44). We remark that the analysis is valid only when the consensus speed is much smaller than the synchronization speed of $\{\omega_i, i \in \mathcal{V}_K\}$. The case when both the synchronization speed of $\{\omega_i, i \in \mathcal{V}_K\}$ and of $\{k_2 \alpha_i \xi_i, i \in \mathcal{V}_K\}$ are fast still needs further consideration.

APPENDIX C STABILITY ANALYSIS OF MLPIAC

In this section, we provide the proof of Theorem (5.6) for MLPIAC. The closed-loop system (34) is rewritten in a vector form as follows,

$$\dot{\tilde{\varphi}} = \omega - \omega_1 1_n, \quad (49a)$$

$$M \dot{\omega} = P - D \omega - P^t + k_2 \alpha^{-1} R \alpha_R \xi, \quad (49b)$$

$$0 = \tilde{P} - \tilde{P}^t, \quad (49c)$$

$$\dot{\eta} = R^T D \omega + k_2 k_3 L \alpha_R \xi, \quad (49d)$$

$$\dot{\xi} = -k_1 (R^T M \omega + \eta) - k_2 \xi, \quad (49e)$$

where $\tilde{\varphi} = \text{col}(\varphi_i)$ with $i \in \mathcal{V}_M \cup \mathcal{V}_F$, $P = \text{col}(P_i) \in \mathbb{R}^n$ for $i \in \mathcal{V}_M \cup \mathcal{V}_F$, $\tilde{P} = \text{col}(P_j) \in \mathbb{R}^{n_p}$ for $j \in \mathcal{V}_P$, $P^t = \text{col}(P_i^t) \in \mathbb{R}^n$ with $P_i^t = \sum_{j \in \mathcal{V}} B_{ij} \sin \varphi_{ij}$ for $i \in \mathcal{V}_M \cup \mathcal{V}_F$, $\tilde{P}^t = \text{col}(\tilde{P}_i^t) \in \mathbb{R}^{n_p}$ with $\tilde{P}_i^t = \sum_{j \in \mathcal{V}} B_{ij} \sin \varphi_{ij}$ for $i \in \mathcal{V}_P$. Note that $\tilde{\varphi}$ only includes the variables $\{\varphi_i, i \in \mathcal{V}_M \cup \mathcal{V}_F\}$ while φ defined in Appendix A includes $\{\varphi_i, i \in \mathcal{V}\}$. For the definitions of M, D, R, α_R , we refer to Appendix A.

We transform the control law (49d,49e) to a new coordinate as a preparation for the stability analysis of DPIAC. Following theorem F.2, let $\rho = Q^{-1}\eta$ and $\sigma = Q^{-1}\xi$. The vector form (49d,49e) becomes

$$\begin{aligned} \dot{\rho} &= Q^{-1} R^T D \omega + k_2 k_3 \Lambda \sigma, \\ \dot{\sigma} &= -k_1 Q^{-1} R^T M \omega - k_1 \rho - k_2 \sigma, \end{aligned}$$

where all the components (ρ_i, σ_i) of (ρ, σ) are decoupled from each other. When writing the dynamics of (ρ_i, σ_i) separately, we derive

$$\dot{\rho}_i = Q_{v_i}^T R^T D\omega + k_2 k_3 \lambda_i \sigma_i, \quad (51a)$$

$$\dot{\sigma}_i = -k_1 Q_{v_i}^T R^T M\omega - k_1 \rho_i - k_2 \sigma_i, \quad (51b)$$

where Q^{-1} is decomposed into vectors, i.e., $Q^{-1} = (Q_{v_1}, Q_{v_2}, \dots, Q_{v_n})$. In (51), the controller of component i calculates the output σ_i with the input ω for the power system. In the following, we investigate the dynamic behavior of the component (ρ_1, σ_1) and $\{(\rho_i, \sigma_i), i = 2, \dots, n\}$ of (ρ, σ) respectively.

For the first component (ρ_1, σ_1) of (ρ, σ) , we have the following lemma.

Lemma C.1: The dynamics of (ρ_1, σ_1) described by (51) is identical to that of (η_s, ξ_s) in (18).

Proof: By (51) and (37b), $\lambda_1 = 0$ and $Q_{v_1} = 1_m$ from (96a), we derive the dynamics of (ρ_1, σ_1) as follows

$$\dot{\rho}_1 = 1_m R^T D\omega = \sum_{i \in \mathcal{V}_M \cup \mathcal{V}_F} D_i \omega_i, \quad (52a)$$

$$\dot{\sigma}_1 = -k_1 (1_m R^T M\omega + \rho_1) - k_2 \sigma_1 \quad (52b)$$

$$= -k_1 \left(\sum_{i \in \mathcal{V}_M} M_i \omega_i + \rho_1 \right) - k_2 \sigma_1. \quad (52c)$$

In addition, by summing all the equations in (49b), (49b) for all $i \in \mathcal{V}$, we derive

$$\begin{aligned} \sum_{i \in \mathcal{V}_M} M_i \dot{\omega}_i &= P_s - \sum_{i \in \mathcal{V}_M \cup \mathcal{V}_F} D_i \omega_i + k_2 1_n^T \alpha^{-1} R \alpha_R \xi \\ &\text{by (37)} \\ &= P_s - \sum_{i \in \mathcal{V}_M \cup \mathcal{V}_F} D_i \omega_i + k_2 1_m^T \xi \\ &\text{by (95a)} \\ &= P_s - \sum_{i \in \mathcal{V}_M \cup \mathcal{V}_F} D_i \omega_i + k_2 \sigma_1. \end{aligned} \quad (53)$$

So $k_2 \sigma_1$ is the control input for the power system (1) as $k_2 \xi_s$. Furthermore, the initial values of (ρ_1, σ_1) and (η_s, ξ_s) are identical, which are both computed from $\{\omega_i(0), i \in \mathcal{V}_K\}$, so the dynamics of (ρ_1, σ_1) is identical to that of (η_s, ξ_s) in (18) if they have the same initial values. \square

We decompose the dynamics of (ρ_i, σ_i) for $i = 2, \dots, m$ into the following two independent dynamics.

$$\begin{aligned} \dot{\rho}_{mi} &= k_2 k_3 \lambda_i \sigma_{mi}, \\ \dot{\sigma}_{mi} &= -k_1 Q_{v_i}^T R^T M\omega - k_1 \rho_{mi} - k_2 \sigma_{mi}, \end{aligned}$$

and

$$\begin{aligned} \dot{\rho}_{di} &= Q_{v_i}^T R^T D\omega + k_2 k_3 \lambda_i \sigma_{di}, \\ \dot{\sigma}_{di} &= -k_1 \rho_{di} - k_2 \sigma_{di}, \end{aligned}$$

from which it can be easily derived that $\rho_i = \rho_{mi} + \rho_{di}$ and $\sigma_i = \sigma_{di} + \sigma_{mi}$.

In the coordinate of $(\varphi, \omega, \rho_1, \sigma_1, \rho_m, \sigma_m, \rho_d, \sigma_d)$, the

closed-loop system (49) becomes

$$\dot{\varphi} = \omega - \omega_1 1_n, \quad (56a)$$

$$M\dot{\omega} = P - D\omega - P^t + k_2 \alpha^{-1} R \alpha_R Q \sigma, \quad (56b)$$

$$0 = \tilde{P} - \tilde{P}^t, \quad (56c)$$

$$\dot{\rho}_1 = 1_m^T R^T D\omega, \quad (56d)$$

$$\dot{\sigma}_1 = -k_1 1_m^T R^T M\omega - k_1 \rho_1 - k_2 \sigma_1, \quad (56e)$$

$$\dot{\rho}_m = k_2 k_3 \Lambda \sigma_m, \quad (56f)$$

$$\dot{\sigma}_m = -k_1 W^T R^T M\omega - k_1 \rho_m - k_2 \sigma_m, \quad (56g)$$

$$\dot{\rho}_d = W^T R^T D\omega + k_2 k_3 \Lambda \sigma_d, \quad (56h)$$

$$\dot{\sigma}_d = -k_1 \rho_d - k_2 \sigma_d, \quad (56i)$$

where $\sigma = \text{col}(\rho_i)$, $\rho_i = \rho_{mi} + \rho_{di}$ for $i = 2, \dots, m$, W is defined as in Theorem (F.2). Note that $\Lambda \in \mathbb{R}^{(m-1) \times (m-1)}$ only includes the nonzero eigenvalues of $L\alpha_R$, which is different from the one in Appendix A.

Following Proposition (5.4), for the closed-loop system (56) we have the following Lemma on the equilibrium state.

Lemma C.2: In the coordinate of $(\varphi, \omega, \rho_1, \sigma_1, \rho_m, \sigma_m, \rho_d, \sigma_d)$, the unique equilibrium state $(\theta^*, \omega^*, \eta^*, \xi^*)$ of the closed-loop system (32) proposed in Proposition (5.4) is equivalent to $(\varphi^*, \omega^*, \rho_1^*, \sigma_1^*, \rho_m^*, \sigma_m^*, \rho_d^*, \sigma_d^*) \in \Phi \times \mathbb{R}^n \times \mathbb{R} \times \mathbb{R} \times \mathbb{R}^{m-1} \times \mathbb{R}^{m-1} \times \mathbb{R}^{m-1} \times \mathbb{R}^{m-1}$ such that

$$\varphi^* \in \Phi = \left\{ \varphi \in \mathbb{R}^{n'} \mid \|\varphi_i - \varphi_j\| < \frac{\pi}{2}, \forall (i, j) \in \mathcal{E}, \varphi_1 = 0 \right\}, \quad (57a)$$

$$\omega_i^* = 0, \quad i \in \mathcal{V}_M \cup \mathcal{V}_F, \quad (57b)$$

$$k_1 \rho_1^* + k_2 \sigma_1^* = 0, \quad (57c)$$

$$k_2 \sigma_1^* + P_s = 0, \quad (57d)$$

$$\rho_{mi}^* = 0, \quad i = 2, \dots, n, \quad (57e)$$

$$\sigma_{mi}^* = 0, \quad i = 2, \dots, n, \quad (57f)$$

$$\rho_{di}^* = 0, \quad i = 2, \dots, n, \quad (57g)$$

$$\sigma_{di}^* = 0, \quad i = 2, \dots, n, \quad (57h)$$

Proof: When mapping θ to φ , we can easily obtain $\varphi \in \Phi = \left\{ \varphi \in \mathbb{R}^{n'} \mid \|\varphi_i - \varphi_j\| < \frac{\pi}{2}, \forall (i, j) \in \mathcal{E}, \varphi_1 = 0 \right\}$, $\omega^* = 0$ can be directly derived from Proposition (5.4).

By Lemma (C.1), we have $(\rho_1^*, \sigma_1^*) = (\eta_s^*, \xi_s^*)$ at the steady state, which yields (57c) and (57d).

By the dynamics (51) of (ρ_{mi}, σ_{mi}) and that of (ρ_{di}, σ_{di}) , we derive that $(\rho_{mi}^*, \sigma_{mi}^*) = (0, 0)$ and $(\rho_{di}^*, \sigma_{di}^*) = (0, 0)$ for all $i = 2, \dots, n$, at the steady state, which lead to (57e)-(57h). \square

In order to prove the asymptotic stability of the equilibrium $(\theta^*, \omega^*, \eta^*, \xi^*)$, we only need to prove the asymptotic stability of the equilibrium $(\varphi^*, \omega^*, \rho_1^*, \sigma_1^*, \rho_m^*, \sigma_m^*, \rho_d^*, \sigma_d^*)$. We define function

$$U(\varphi) = \sum_{(i,j) \in \mathcal{E}} B_{ij} (1 - \cos(\varphi_i - \varphi_j)) \quad (58)$$

and variable $v_s = \sum_{i \in \mathcal{V}_M} M_i \omega_i + \rho_1$. By (53) and (52), we obtain dynamics of (v_s, σ_1) ,

$$\dot{v}_s = P_s + k_2 \sigma_1, \quad (59a)$$

$$\dot{\sigma}_1 = -k_1 v_s - k_2 \sigma_1, \quad (59b)$$

with equilibrium state $(v_s^*, \sigma_1^*) = (\frac{1}{k_1} P_s, -\frac{1}{k_2} P_s)$.

In the following, we prove the equilibrium $(\theta^*, \omega^*, \rho_1^*, \sigma_1^*, \rho_m^*, \sigma_m^*, \rho_d^*, \sigma_d^*)$ is locally asymptotically stable following Lyapunov method.

Proof of Theorem (5.6): The existence and uniqueness of the synchronous state in Ψ follows Proposition (5.4) directly. Since the closed-loop system (32) is equivalent to (56), we prove the equilibrium $(\varphi^*, \omega^*, \rho_1^*, \sigma_1^*, \rho_m^*, \sigma_m^*, \rho_d^*, \sigma_d^*)$ of (56) is locally asymptotically stable. The proof follows Theorem (E.3). It follows [40, Lemma 5.2] that the algebraic equations (34d) are regular. In addition, there exists a unique equilibrium for the closed-loop system (56) following Lemma (C.2), we only need to find a Lyapunov function $V(x, y)$ as in Theorem (E.3).

Before introducing the Lyapunov function candidate, we define the following functions.

$$\begin{aligned} V_0 &= U(\varphi) - U(\varphi^*) - \nabla_{\varphi} U(\varphi^*)(\varphi - \varphi^*) + \frac{1}{2} \omega^T M \omega, \\ V_1 &= (c_1 + 1) \left(\frac{1}{2k_1} (k_1 v_s - k_1 v_s^*)^2 + \frac{1}{2k_2} (k_2 \sigma_1 - k_2 \sigma_1^*)^2 \right) \\ &\quad + \frac{1}{2k_2} (k_2 \sigma_1 - k_2 \sigma_1^*)^2 + \frac{1}{2k_1} (k_1 v_s + k_2 \sigma_1)^2, \end{aligned}$$

where $c_1 \in \mathbb{R}$ and $k_1 v_s^* + k_2 \sigma_1^* = 0$ has been used. Denote $x_m = k_1 \rho_m$, $y_m = k_2 \sigma_m$, $z_m = k_1 \rho_m + k_2 \sigma_m$, $x_d = k_1 \rho_d$, $y_d = k_2 \sigma_d$, $z_d = k_1 \rho_d + k_2 \sigma_d$ and define

$$\begin{aligned} V_m &= \frac{\beta_m}{2} x_m^T C_m x_m + \frac{(1 + \beta_m) k_1 k_3}{2k_2} y_m^T C_m \Lambda y_m + \frac{1}{2} z_m^T C_m z_m, \\ V_d &= \frac{\beta_d c_d}{2} x_d^T x_d + \frac{(1 + \beta_d) c_d k_1 k_3}{2k_2} y_d^T \Lambda y_d + \frac{c_d}{2} z_d^T z_d, \end{aligned}$$

where $\beta_m \in \mathbb{R}$, $\beta_d \in \mathbb{R}$, $c_d \in \mathbb{R}$ are positive and $C_m = \text{diag}(c_{mi}) \in \mathbb{R}^{(m-1) \times (m-1)}$ with all the diagonal elements $c_{mi} > 0$, and $\Lambda \in \mathbb{R}^{(m-1) \times (m-1)}$ is a diagonal matrix with diagonal elements being the nonzero eigenvalues of $L\alpha_R$.

In the following, we focus on the derivatives of the functions V_0, V_1, V_m, V_d . The derivative of V_0 is

$$\begin{aligned} \dot{V}_0 &= -\omega^T D \omega + (k_2 \sigma - k_2 \sigma^*)^T Q^T \alpha_R R^T \alpha^{-1} \omega \\ &\quad \text{by } Q = [Q_1, Q_2, \dots, Q_n] \text{ and } S = [Q_2, \dots, Q_n]. \\ &= -\omega^T D \omega + (k_2 \sigma_1 - k_2 \sigma_1^*) Q_1^T \alpha_R R^T \alpha^{-1} \omega \\ &\quad + (k_2 \sigma - k_2 \sigma^*)^T S^T \alpha_R R^T \alpha^{-1} \omega \\ &= -\omega^T D \omega + (k_2 \sigma_1 - k_2 \sigma_1^*) Q_1^T \alpha_R R^T \alpha^{-1} \omega \\ &\quad + (k_2 \sigma_m - k_2 \sigma_m^*)^T S^T \alpha_R R^T \alpha^{-1} \omega \\ &\quad + (k_2 \sigma_d - k_2 \sigma_d^*)^T S^T \alpha_R R^T \alpha^{-1} \omega, \\ &\quad \text{by } S^T \alpha_R = W^T, Q_1^T \alpha_R = Q_{v_1}^T, \sigma_m^* = 0 \\ &= -\omega^T D \omega + (k_2 \sigma_1 - k_2 \sigma_1^*) Q_{v_1}^T R^T \alpha^{-1} \omega \\ &\quad + (k_2 \sigma_m)^T W^T R^T \alpha^{-1} \omega + (k_2 \sigma_d)^T W^T R^T \alpha^{-1} \omega \\ &= -\omega^T D \omega + (k_2 \sigma_1 - k_2 \sigma_1^*) Q_{v_1}^T R^T \alpha^{-1} \omega \\ &\quad + y_m^T W^T R^T \alpha^{-1} \omega + y_d^T W^T R^T \alpha^{-1} \omega. \end{aligned}$$

The derivative of V_1 is

$$\begin{aligned} \dot{V}_1 &= -(c_1 + 1)(k_2 \sigma_1 - k_2 \sigma_1^*)^2 - \frac{k_2}{k_1} (k_1 v + k_2 \sigma_1)^2 \\ &\quad \text{plus a term and minus it} \\ &= -(k_2 \sigma_1 - k_2 \sigma_1^*) Q_{v_1}^T R^T \alpha^{-1} \omega \\ &\quad + (k_2 \sigma_1 - k_2 \sigma_1^*) Q_{v_1}^T R^T \alpha^{-1} \omega \\ &\quad - (c_1 + 1)(k_2 \sigma_1 - k_2 \sigma_1^*)^2 - \frac{k_2}{k_1} (k_1 v + k_2 \sigma_1)^2. \end{aligned}$$

By inequalities

$$\begin{aligned} (k_2 \sigma_1 - k_2 \sigma_1^*) Q_{v_1}^T R^T \alpha^{-1} \omega &\leq \frac{1}{8} \omega^T \epsilon D \omega \\ &\quad + 2(k_2 \sigma_1 - k_2 \sigma_1^*)^2 Q_{v_1}^T R^T \alpha^{-2} (\epsilon D)^{-1} R Q_{v_1}, \end{aligned}$$

we obtain

$$\begin{aligned} \dot{V}_1 &\leq -(k_2 \sigma_1 - k_2 \sigma_1^*) Q_{v_1}^T R^T \alpha^{-1} \omega + \frac{1}{8} \omega^T \epsilon D \omega \\ &\quad + 2(k_2 \sigma_1 - k_2 \sigma_1^*)^2 Q_{v_1}^T R^T \alpha^{-2} (\epsilon D)^{-1} R Q_{v_1} \\ &\quad - (c_1 + 1)(k_2 \sigma_1 - k_2 \sigma_1^*)^2 - \frac{k_2}{k_1} (k_1 v_s + k_2 \sigma_1)^2 \\ &\quad \text{let } c_1 = 2Q_{v_1}^T R^T \alpha^{-2} (\epsilon D)^{-1} R Q_{v_1} \\ &= -(k_2 \sigma_1 - k_2 \sigma_1^*) Q_{v_1}^T R^T \alpha^{-1} \omega + \frac{1}{8} \omega^T \epsilon D \omega \\ &\quad - (k_2 \sigma_1 - k_2 \sigma_1^*)^2 - \frac{k_2}{k_1} (k_1 v + k_2 \sigma_1)^2. \end{aligned}$$

The derivative of V_m is

$$\begin{aligned} \dot{V}_m &= -k_2 z_m^T C_m z_m - \beta_m k_1 k_3 y_m^T C_m \Lambda y_m \\ &\quad - k_1 k_2 z_m^T C_m W^T R^T M \omega \\ &\quad - (1 + \beta_m) k_1^2 k_3 y_m^T C_m \Lambda W^T R^T M \omega \\ &= -y_m^T W^T R^T \alpha^{-1} \omega + y_m^T W^T R^T \alpha^{-1} \omega - k_2 z_m^T C_m z_m \\ &\quad - \beta_m k_1 k_3 y_m^T C_m \Lambda y_m - k_1 k_2 z_m^T C_m W^T R^T M \omega \\ &\quad - (1 + \beta_m) k_1^2 k_3 y_m^T C_m \Lambda W^T R^T M \omega \\ &= -y_m^T W^T R^T \alpha^{-1} \omega + \sum_{i=2}^n y_{mi} Q_{vi}^T R^T \alpha^{-1} \omega - k_2 \sum_{i=2}^n c_{mi} z_{mi}^2 \\ &\quad - \beta_m k_1 k_3 \sum_{i=2}^n c_{mi} \lambda_i y_{mi}^2 - k_1 k_2 \sum_{i=2}^n c_{mi} z_{mi} Q_{vi}^T R^T M \omega \\ &\quad - (1 + \beta_m) k_1^2 k_3 \sum_{i=2}^n \left(c_{mi} \lambda_i y_{mi} Q_{vi}^T R^T M \omega \right) \\ &= -y_m^T W^T R^T \alpha^{-1} \omega - k_2 \sum_{i=2}^n c_{mi} z_{mi}^2 - \beta_m k_1 k_3 \sum_{i=2}^n c_{mi} \lambda_i y_{mi}^2 \\ &\quad - k_1 k_2 \sum_{i=2}^n \left(c_{mi} z_{mi} Q_{vi}^T R^T M \omega \right) \\ &\quad + \sum_{i=2}^n y_{mi} (Q_{vi}^T R^T \alpha^{-1} - Q_{vi}^T (1 + \beta_m) k_1^2 k_3 c_{mi} \lambda_i R^T M) \omega. \end{aligned}$$

By the following inequalities

$$k_1 k_2 c_{mi} z_{mi} Q_{vi}^T R^T M \omega \leq \frac{\omega^T \epsilon D \omega}{8(n-1)} + r_m z_{mi}^2,$$

where $r_z = 2(n-1)(k_1 k_2 c_{mi})^2 Q_{vi}^T R^T (D\epsilon)^{-1} M^2 R Q_{vi}$, and

$$y_{mi} Q_{vi}^T R^T (\alpha^{-1} - (1 + \beta_m) k_1^2 k_3 c_{mi} \lambda_i M) \omega \leq \frac{\omega^T \epsilon D \omega}{8(n-1)} + r_z y_{mi}^2,$$

where

$$r_y = 2(n-1) Q_{vi}^T R^T ((\alpha^{-1} - (1 + \beta_m) k_1^2 k_3 c_{mi} \lambda_i M)^2 (\epsilon D)^{-1} R Q_{vi}),$$

we obtain

$$\begin{aligned} \dot{V}_m &\leq -y_m^T W^T R^T \alpha^{-1} \omega + \frac{1}{4} \omega^T \epsilon D \omega - \sum_{i=2}^n z_{mi}^2 (k_2 c_{mi} - r_z) \\ &\quad - \sum_{i=2}^n y_{mi}^2 (\beta_m k_1 k_3 c_{mi} \lambda_i - r_y). \end{aligned}$$

The derivative of V_d is

$$\begin{aligned} \dot{V}_d &= -c_d k_2 z_d^T z_d - y_d^T (c_d \beta_d k_1 k_3 \Lambda) y_d \\ &\quad + z_d^T ((1 + \beta_d) c_d k_1) W^T R^T D \omega \\ &\quad - y_d^T (\beta_d c_d k_1 I_{n-1}) W^T R^T D \omega \\ &= -y_d^T W^T R^T \alpha^{-1} \omega + y_d^T W^T R^T \alpha^{-1} \omega - c_d k_2 z_d^T z_d \\ &\quad - y_d^T (c_d \beta_d k_1 k_3 \Lambda) y_d + z_d^T ((1 + \beta_d) c_d k_1) W^T R^T D \omega \\ &\quad - y_d^T (\beta_d c_d k_1) W^T R^T D \omega \\ &= -y_d^T W^T R^T \alpha^{-1} \omega - c_d k_2 z_d^T z_d - y_d^T (c_d \beta_d k_1 k_3 \Lambda) y_d \\ &\quad + z_d^T ((1 + \beta_d) c_d k_1) W^T R^T D \omega \\ &\quad + y_d^T W^T R^T (\alpha^{-1} - \beta_d c_d k_1 D) \omega. \end{aligned}$$

By $\lambda_{\min} \leq \lambda_i$ for all $i = 2, \dots, n$, and inequalities

$$z_d^T W^T R^T ((1 + \beta_d) c_d k_1) D \omega \leq \frac{1}{2} \omega^T D \omega^T + \frac{1}{2} z_d^T X_z z_d,$$

where $X_z = W^T R^T ((1 + \beta_d) c_d k_1 \alpha D)^2 D^{-1} R W$, and

$$y_d^T W^T R^T (\alpha^{-1} - \beta_d c_d k_1 D) \omega \leq \frac{1}{2} \omega^T (D - \epsilon D) \omega + \frac{1}{2} y_d^T X_y y_d,$$

where $X_y = W^T R^T (\alpha^{-1} - \beta_d c_d k_1 D)^2 (D - \epsilon D)^{-1} R W$, we derive,

$$\begin{aligned} \dot{V}_d &\leq -y_d^T W^T R^T \alpha^{-1} \omega - c_d k_2 z_d^T z_d - c_d \beta_d k_1 k_3 \lambda_{\min} y_d^T y_d \\ &\quad + z_d^T W^T R^T ((1 + \beta_d) c_d k_1) D \omega \\ &\quad + y_d^T W^T R^T (\alpha^{-1} - \beta_d c_d k_1 D) \omega \\ &\leq -y_d^T W^T R^T \omega + \omega^T D \omega - \frac{1}{2} \omega^T \epsilon D \omega \\ &\quad - z_d^T (c_d k_2 - \frac{1}{2} X_z) z_d - y_d^T (c_d \beta_d k_1 k_3 \lambda_{\min} - \frac{1}{2} X_y) y_d. \end{aligned}$$

We consider the following Lyapunov function candidate,

$$V = V_0 + V_1 + V_m + V_d.$$

In the following, we prove that (i) $\dot{V} \leq 0$, (ii) equilibrium $z^* = (\varphi^*, \omega^*, \rho_1^*, \sigma_1^*, \rho_m^*, \sigma_m^*, \rho_d^*, \sigma_d^*)$ is a strict minimum of $V(\cdot)$ such that $\nabla V|_{z^*} = 0$ and $\nabla^2 V|_{z^*} > 0$, and (iii) z^* is the only isolated equilibrium in the invariant set $\{z \in \Phi \times \mathbb{R}^n \times \mathbb{R} \times \mathbb{R} \times \mathbb{R}^{m-1} \times \mathbb{R}^{m-1} \times \mathbb{R}^{m-1} \times \mathbb{R}^{m-1} | \dot{V}(z) = 0\}$ step by step according to Theorem (E.3).

(i). V has derivative

$$\dot{V} \leq G_0 + G_1 + G_m + G_d, \quad (75)$$

where the terms $y_m^T W^T R^T \alpha^{-1} \omega$, $y_d^T W^T R^T \alpha^{-1} \omega$ have vanished and the terms G_0, G_1, G_m, G_d are mainly from $\dot{V}_0, \dot{V}_1, \dot{V}_m, \dot{V}_d$ respectively with the following form,

$$G_0 = -\frac{1}{8} \omega^T \epsilon D \omega,$$

$$G_1 = -(k_2 \sigma_1 - k_2 \sigma_1^*)^2 - \frac{k_2}{k_1} (k_1 u + k_2 \sigma_1)^2,$$

$$G_m = -\sum_{i=2}^n z_{mi}^2 (c_{mi} k_2 - r_z) - \sum_{i=2}^n y_{mi}^2 (\beta_m k_1 k_3 c_{mi} \lambda_i - r_y),$$

$$G_d = -z_d^T (c_d k_2 - \frac{1}{2} X_z) z_d - y_d^T (c_d \beta_d k_1 k_3 \lambda_{\min} - \frac{1}{2} X_y) y_d.$$

It is obvious that $G_0 \leq 0$ and $G_1 \leq 0$. In the following, we first focus on G_m and then on G_d . If there exist c_{mi} and β_m such that $c_{mi} k_2 - r_z > 0$ and $\beta_m k_1 k_3 c_{mi} \lambda_i - r_y > 0$, we have $G_m \leq 0$ for all z_m and y_m . We verify that such c_{mi} and β_m do exist. By (37a) and (96b), we have

$$Q_{vi}^T R^T \alpha^{-1} R Q_{vi} = Q_{vi}^T \alpha_R^{-1} Q_{vi} = 1.$$

So we only need to prove there exist c_{mi} and β_m such that

$$\begin{aligned} Q_{vi}^T R^T (c_{mi} k_2 \alpha^{-1}) R Q_{vi} - r_z &> 0, \\ Q_{vi}^T R^T (\beta_m k_1 k_3 c_{mi} \lambda_i \alpha^{-1}) R Q_{vi} - r_y &> 0, \end{aligned}$$

which yields

$$\begin{aligned} c_{mi} k_2 \alpha^{-1} &> 2(n-1)(c_{mi} k_1 k_2 M)^2 (\epsilon D)^{-1}, \quad (79a) \\ (\beta_m k_1 k_3 c_{mi} \lambda_i \alpha^{-1}) &> 2(n-1)(\alpha^{-1} - c_{mi}(1 + \beta_m) k_1 k_3 \lambda_i M)^2 (\epsilon D)^{-1}, \quad (79b) \end{aligned}$$

From (79), we derive

$$\begin{aligned} c_{mi} I_{m-1} &< \frac{\epsilon D}{2(n-1)k_1^2 k_2 M^2 \alpha}, \\ \frac{I_{m-1}}{2a + b + \sqrt{4ab + b^2}} &< c_{mi} I_{m-1} < \frac{2a + b + \sqrt{4ab + b^2}}{2a^2}, \end{aligned}$$

where $a = (1 + \beta_m) k_1^2 k_3 \lambda_i M \alpha$, $b = \frac{\beta_m k_1 k_3 \alpha \lambda_i \epsilon D}{2(n-1)}$. There exists $c_{mi} > 0$ satisfying (79) if

$$\left(\frac{I_{n-1}}{2a + b + \sqrt{4ab + b^2}} \right)_{\max} < \left(\frac{\epsilon D}{2(n-1)k_1^2 k_2 M^2 \alpha} \right)_{\min}$$

which can be satisfied by choosing a large β_m . This is because

$$\lim_{\beta_m \rightarrow \infty} \left(\frac{1}{2a + b + \sqrt{4ab + b^2}} \right)_{\max} = 0,$$

while the term $\left(\frac{\epsilon D}{2(n-1)k_1^2 k_2 M^2 \alpha} \right)_{\min}$ does not depend on β_m . Hence there exist $c_{mi} > 0$ and $\beta_m > 0$ satisfying (79) and $G_m \leq 0$ has been proven. Here $(\cdot)_{\max}$ and $(\cdot)_{\min}$ are as defined in Assumption (5.5).

In the following, we focus on G_d . If there exist c_d and β_d such that

$$c_d k_2 I_{m-1} - \frac{1}{2} X_z > 0,$$

$$c_d \beta_d k_1 k_3 \lambda_{\min} I_{m-1} - \frac{1}{2} X_y > 0,$$

we have $G_d \leq 0$. We prove such c_d and β_d do exist with

Assumption (5.5). By (37a) and (96b), we derive

$$W^T R^T \alpha^{-1} R W = W^T \alpha_R^{-1} W = I_{m-1}.$$

So we only need to prove there exist c_d and β_d such that

$$\begin{aligned} W^T R^T (c_d k_2 \alpha^{-1}) R W - \frac{1}{2} X_z &> 0, \\ W^T R^T (c_d \beta_d k_1 k_3 \lambda_{\min}) R W - \frac{1}{2} X_y &> 0, \end{aligned}$$

which yields

$$c_d k_2 \alpha^{-1} > \frac{1}{2} (1 + \beta_d)^2 (c_d k_1 D)^2 D^{-1}, \quad (86a)$$

$$c_d \beta_d k_1 k_3 \lambda_{\min} \alpha^{-1} > \frac{1}{2} (\alpha^{-1} - \beta_d c_d k_1 D)^2 (D - \epsilon D)^{-1}, \quad (86b)$$

In the following, we prove that with assumption (5.5), there exist c_d and β_d satisfying the above two inequalities (86). We derive from (86) that

$$\begin{aligned} c_d I_{m-1} &< \frac{2k_2}{(1 + \beta_d)^2 k_1^2 \alpha D}, \\ \frac{1}{\beta_d k_1 \alpha D b_d} &< c_d I_{m-1} < \frac{b_d}{\beta_d k_1 \alpha D}, \end{aligned}$$

where

$$b_d = 1 + k_3 \lambda_{\min} (1 - \epsilon) + \sqrt{k_3^2 \lambda_{\min}^2 (1 - \epsilon)^2 + 2k_3 \lambda_{\min} (1 - \epsilon)}.$$

There exists a c_d satisfying the two inequalities (86) if there exists a β_d such that

$$\frac{1}{\beta_d k_1 (\alpha D)_{\min} b_d} < \frac{2k_2}{(1 + \beta_d)^2 k_1^2 (\alpha D)_{\max}}. \quad (88)$$

Since

$$\begin{aligned} \lim_{\epsilon \rightarrow 0} b_d(\epsilon) &= 1 + k_3 \lambda_{\min} + \sqrt{k_3^2 \lambda_{\min}^2 + 2k_3 \lambda_{\min}} \\ &> 1 + 2k_3 \lambda_{\min}, \end{aligned}$$

there exists a small $\epsilon > 0$ such that $b_d(\epsilon) > 1 + 2k_3 \lambda_{\min}$. Subsequently (88) can be satisfied if

$$\frac{1}{\beta_d k_1 (\alpha D)_{\min} (1 + 2k_3 \lambda_{\min})} < \frac{2k_2}{(1 + \beta_d)^2 k_1^2 (\alpha D)_{\max}}. \quad (90)$$

With assumption (5.5), we can obtain that there exist $\beta_d > 0$ satisfying (90). Hence $G_d < 0$ is proven and $\dot{V} \leq 0$ subsequently.

(ii). We prove that the equilibrium z^* is a strict minimum of $V(\cdot)$. It can be easily verified that $V|_{z^*} = 0$ and

$$\nabla V|_{z^*} = \text{col}(\nabla_{\varphi} V, \nabla_{\tilde{z}} V)|_{z^*} = 0,$$

where $\tilde{z} = (\omega, \rho_1 - \rho_1^*, \sigma_1 - \sigma_1^*, \rho_m, \sigma_m, \rho_d, \sigma_d)$. Here, we have used $(\omega^*, \rho_m^*, \sigma_m^*, \rho_d^*, \sigma_d^*) = 0$. The Hessian matrix of V at z^* is

$$\nabla^2 V|_{z^*} = \text{blkdiag}(L_p, H),$$

where L_p is Hessian matrix of V respect to φ with $\varphi_1 = 0$ and H is the Hessian matrix of V respect to \tilde{z} . It follows [40, Lemma 5.3] that L is positive definite. Since the components in V related to \tilde{z} are all quadratic and positive definite, H is positive definite. Thus $\nabla^2 V|_{z^*} > 0$.

(iii). The equilibrium is the only isolated one in the invariant set $\{(\varphi, \omega, \eta_m, \xi_m, \eta_d, \xi_d) | \dot{V} = 0\}$. Since $\dot{V} = 0$, it yields from (75) that $\tilde{z} = 0$. Hence φ_i are all constant. By Proposition (5.4), we prove that z^* is the only isolated equilibrium in the invariant set.

In this case, z^* is the only one equilibrium in the neighborhood of z^* such that $\Psi^d = \{(\varphi, \tilde{z}) | V(\varphi, \tilde{z}) \leq c, \varphi \in \Phi\}$ for some $c > 0$. Hence with any initial state z^0 that satisfies the algebraic equations (34d), the trajectory converges to the equilibrium state z^* . \square

Remark C.3: Note that when the power system is controlled as a single region, MLPIAC reduces to GBPIAC. The dynamics of $(\rho_m, \sigma_m, \rho_d, \sigma_d)$ vanish and the one of (ρ_1, σ_1) is left only. In the Lyapunov function $V(\cdot)$, with $V_m = 0$ and $V_d = 0$, we can prove the equilibrium of GBPIAC is locally asymptotically stable without Assumption (5.5).

APPENDIX D

THE OPTIMAL CONTROL FRAMEWORK OF ODES

Consider the following optimal control problem of a *Differential Algebraic Equation* (DAE) system [19],

$$\min_{u_i \in \mathbb{R}} \int_0^{T_0} u^T(t) R_1 u(t) + x(t)^T R_2 x(t) dt \quad (91a)$$

$$\text{s.t.} \quad \dot{x} = f(x, y, u), \quad (91b)$$

$$0 = g(x, y, u), \quad (91c)$$

with the initial condition $(x(0), y(0), u(0)) = (x_0, y_0, u_0)$ such that $g(x_0, y_0, u_0) = 0$. Here, $x \in \mathbb{R}^n, y \in \mathbb{R}^m, u \in \mathbb{R}^z$ are the state variable, algebraic variable and control input respectively, and $f : \mathbb{R}^n \times \mathbb{R}^m \times \mathbb{R}^z \rightarrow \mathbb{R}^n$ and $g : \mathbb{R}^n \times \mathbb{R}^m \times \mathbb{R}^z \rightarrow \mathbb{R}^m$. The matrix $R_1 \in \mathbb{R}^z \times \mathbb{R}^z$ and $R_2 \in \mathbb{R}^n \times \mathbb{R}^n$. $R_1 = R_1^T > 0$ and $R_2 = R_2^T > 0$ determine the trade-off between the control input and the state oscillations.

APPENDIX E

PRELIMINARIES ON DAEs

Consider the following DAE systems

$$\dot{x} = f(x, y), \quad (92a)$$

$$0 = g(x, y), \quad (92b)$$

where $x \in \mathbb{R}^n, y \in \mathbb{R}^m$ and $f : \mathbb{R}^n \times \mathbb{R}^m \rightarrow \mathbb{R}^n$ and $g : \mathbb{R}^n \times \mathbb{R}^m \rightarrow \mathbb{R}^m$ are twice continuously differentiable functions. $(x(x_0, y_0, t), y(x_0, y_0, t))$ is the solution with the admissible initial conditions (x_0, y_0) satisfying the algebraic constraints

$$0 = g(x_0, y_0), \quad (93)$$

and the maximal domain of a solution of (92) is denoted by $\mathcal{I} \subset \mathbb{R}_{\geq 0}$ where $\mathbb{R}_{\geq 0} = \{x \in \mathbb{R} | x \geq 0\}$.

Before presenting the Lyapunov/LaSalle stability criterion of the DAE system, we make the following two assumptions.

Assumption E.1: The DAE system possesses an equilibrium state (x^*, y^*) such that $f(x^*, y^*) = 0, g(x^*, y^*) = 0$.

Assumption E.2: Let $\Omega \subseteq \mathbb{R}^n \times \mathbb{R}^m$ be an open connected set containing (x^*, y^*) , assume (92b) is *regular* such that the

Jacobian of g with respect to y is a full rank matrix for any $(x, y) \in \Omega$, i.e.,

$$\text{rank}(\nabla_y g(x, y)) = m, \quad \forall (x, y) \in \Omega.$$

Assumption (E.2) ensures the existence and uniqueness of the solutions of (92) in Ω over the interval \mathcal{I} with the initial condition (x_0, y_0) satisfying (93).

The following theorem provides a sufficient stability criterion of the equilibrium of DAE in (92).

Theorem E.3: (Lyapunov/LaSalle stability criterion [26], [13]): Consider the DAE system in (92) with assumptions (E.1) and (E.2), and an equilibrium $(x^*, y^*) \in \Omega_H \subset \Omega$. If there exists a continuously differentiable function $H : \Omega_H \rightarrow \mathbb{R}$, such that (x^*, y^*) is a strict minimum of H i.e., $\nabla H|_{(x^*, y^*)} = 0$ and $\nabla^2 H|_{(x^*, y^*)} > 0$, and $\dot{H}(x, y) \leq 0$, $\forall (x, y) \in \Omega_H$, then the following statements hold:

(1). (x^*, y^*) is a stable equilibrium with a local Lyapunov function $V(x, y) = H(x, y) - H(x^*, y^*) \geq 0$ for (x, y) near (x^*, y^*) ,

(2). Let $\Omega_c = \{(x, y) \in \Omega_H | H(x, y) \leq c\}$ be a compact sub-level set for a $c > H(x^*, y^*)$. If no solution can stay in $\{(x, y) \in \Omega_c | \dot{H}(x, y) = 0\}$ other than (x^*, y^*) , then (x^*, y^*) is asymptotically stable.

We refer to [26] and [13] for the proof of Theorem E.3.

APPENDIX F

PRELIMINARIES OF SYMMETRIZABLE MATRIX

In this section, we introduce the properties of a *symmetrizable matrix* defined as follows.

Definition F.1: A matrix $B \in \mathbb{R}^{m \times m}$ is *symmetrizable* if there exists a positive-definite invertible diagonal matrix $A \in \mathbb{R}^{m \times m}$ and a symmetric matrix $L \in \mathbb{R}^{m \times m}$ such that $B = LA$.

Theorem F.2: Consider the Laplacian matrix $L \in \mathbb{R}^{m \times m}$ as defined in (26) and the positive-definite diagonal matrix $\alpha_R \in \mathbb{R}^{m \times m}$ as defined in Appendix (A). The matrix $L\alpha_R$ is a symmetrizable matrix and there exists an invertible matrix Q such that

$$Q^{-1}L\alpha_R Q = \Lambda, \quad (94)$$

where $\Lambda = \text{diag}(\lambda_i) \in \mathbb{R}^{m \times m}$, λ_i is the eigenvalue of $L\alpha$ and $\lambda_1 = 0$. Denote $Q^{-1} = [Q_{v1}, Q_{v2}, \dots, Q_{vm}]^T$ and $Q = [Q_1, Q_2, \dots, Q_m]$, we have

$$Q_{v1} = 1_m, \quad (95a)$$

$$\alpha_R Q_1 = 1_m, \quad (95b)$$

$$Q^T \alpha_R Q = I_m, \quad (95c)$$

$$Q^{-1} \alpha_R^{-1} (Q^{-1})^T = I_m, \quad (95d)$$

$$Q^{-1} = Q^T \alpha_R. \quad (95e)$$

Furthermore, the new matrix $W = [Q_{v2}, \dots, Q_{vm}] \in \mathbb{R}^{n \times (m-1)}$ and $S = [Q_2, \dots, Q_m] \in \mathbb{R}^{m \times (m-1)}$ satisfy that

$$W^T S = I_{(m-1)}, \quad (96a)$$

$$W^T \alpha_R^{-1} W = I_{(m-1)}, \quad (96b)$$

$$S^T \alpha_R S = I_{(m-1)}, \quad (96c)$$

$$Q_{vi} = \alpha_R Q_i, \quad (96d)$$

$$W = \alpha_R S. \quad (96e)$$

Proof: Let $T = \sqrt{\alpha_R}$ which is a diagonal matrix, then

$$TL\alpha_R T^{-1} = \sqrt{\alpha_R} L \sqrt{\alpha_R}.$$

Hence, there exists an invertible matrix $\Gamma^{-1} = \Gamma^T$ such that

$$\Gamma^{-1} TL\alpha_R T^{-1} \Gamma = \Gamma^{-1} \sqrt{\alpha_R} L \sqrt{\alpha_R} \Gamma = \Lambda.$$

Let $Q = T^{-1} \Gamma$, we derive $Q^{-1} L \alpha_R Q = \Lambda$. Since L is a Laplacian matrix as defined in (26), we have $1_m^T L \alpha_R = 0$, then there is a zero eigenvalue, i.e., $\lambda_1 = 0$. Denote $\Gamma = [\Gamma_1, \Gamma_2, \dots, \Gamma_m]$, then $\Gamma^{-1} = \Gamma^T = [\Gamma_1, \Gamma_2, \dots, \Gamma_m]^T$.

Since Γ_1 is the eigenvector corresponding to $\lambda_1 = 0$ of $\sqrt{\alpha_R} L \sqrt{\alpha_R}$ such that $L \sqrt{\alpha_R} \Gamma_1 = 0$, from which we derive $\sqrt{\alpha_R} \Gamma_1 = 1_m$. Hence by $Q = T^{-1} \Gamma$, we obtain $Q_1 = (\sqrt{\alpha_R})^{-1} \Gamma_1 = \alpha_R^{-1} 1_m$. Similarly we derive $Q_{v1} = \Gamma_1^T T = \Gamma^T \sqrt{\alpha_R} = \sqrt{\alpha_R} \Gamma_1 = 1_m$.

By $Q = T^{-1} \Gamma$, we derive $\Gamma^T \alpha_R Q = \Gamma^T T^{-1} \alpha_R T^{-1} \Gamma = I_m$. $Q^{-1} \alpha_R^{-1} (Q^{-1})^T = R^T R = I_m$ can be obtained similarly.

(96a) is yielded directly from $Q^{-1} Q = I_m$. (95c) and (95d) yields (96b) and (96c). \square

APPENDIX G

\mathcal{H}_2 NORM IN LINEAR INPUT/OUTPUT SYSTEMS

The \mathcal{H}_2 norm of the transfer matrix of a linear system is defined as follows.

Definition G.1: Consider a linear time-invariant system,

$$\dot{x} = Ax + Bw, \quad (97a)$$

$$y = Cx, \quad (97b)$$

where $x \in \mathbb{R}^n$, $A \in \mathbb{R}^{n \times n}$ is Hurwitz, $B \in \mathbb{R}^{n \times m}$, $C \in \mathbb{R}^{z \times n}$, the input is denoted by $w \in \mathbb{R}^m$ and the output of the system is denoted by $y \in \mathbb{R}^z$. The squared \mathcal{H}_2 norm of the transfer matrix H of the map (A, B, C) from the input w to the output y is defined as

$$\|H\|_2^2 = \text{tr}(B^T Q_o B) = \text{tr}(C Q_c C^T), \quad (98a)$$

$$Q_o A + A^T Q_o + C^T C = 0, \quad (98b)$$

$$A Q_c + Q_c A^T + B B^T = 0, \quad (98c)$$

where $\text{tr}(\cdot)$ is the trace of a matrix, $Q_o, Q_c \in \mathbb{R}^{n \times n}$ are the *observability Gramian* of (C, A) and *controllability Gramian* of (A, B) respectively [10],[33, chapter 2].

There are several interpretations of the \mathcal{H}_2 norm. When the input w is modeled as the Gaussian white noise such that $w_i \sim N(0, 1)$ for all $i = 1, \dots, m$, the matrix $Q_v = C Q_c C^T$ is the variance matrix of the output at the steady state, i.e.,

$$Q_v = \lim_{t \rightarrow \infty} E[y(t)y^T(t)]$$

where $E[\cdot]$ denotes the expectation. Thus

$$\|H\|_2^2 = \text{tr}(Q_v) = \lim_{t \rightarrow \infty} E[y(t)^T y(t)]. \quad (99)$$

When the input w is modeled as Dirac impulse with $w(t) = e_i \delta(t)$ where $e_i \in \mathbb{R}^m$ is a vector with the i th component being one and others zero, and $\delta(t)$ is a Dirac impulse. The

corresponding output to $e_i\delta(t)$ is denoted by $y_i \in \mathbb{R}^z$ for $i = 1, \dots, m$. Then the squared \mathcal{H}_2 norm satisfies [32]

$$\|H\|_2^2 = \sum_{i=1}^m \int_0^\infty y_i(t)^T y_i(t) dt. \quad (100)$$

which measures the sum of the \mathcal{L}_2 norm of the outputs.

The \mathcal{H}_2 norm can also be interpreted as the expected \mathcal{L}_2 norm of the output y with $w = 0$ and a random initial condition x_0 such that $E[x_0 x_0^T] = BB^T$, or equivalently,

$$\|H\|_2^2 = \int_0^\infty E[y^T(t)y(t)] dt. \quad (101)$$

The \mathcal{H}_2 norm has been often used to investigate the performance of secondary frequency control methods, e.g., [2], [29], [37], to study the optimal virtual inertia placement in Micro-Grids [25] and the price of the synchrony of power systems [32].